

This is an Open Access document downloaded from ORCA, Cardiff University's institutional repository: <https://orca.cardiff.ac.uk/id/eprint/108986/>

This is the author's version of a work that was submitted to / accepted for publication.

Citation for final published version:

Alves, Tiago M. and Cupkovic, Tomas 2018. Footwall degradation styles and associated sedimentary facies distribution in SE Crete: Insights into tilt-block extensional basins on continental margins. *Sedimentary Geology* 10.1016/j.sedgeo.2018.02.001

Publishers page: <http://dx.doi.org/10.1016/j.sedgeo.2018.02.001>

Please note:

Changes made as a result of publishing processes such as copy-editing, formatting and page numbers may not be reflected in this version. For the definitive version of this publication, please refer to the published source. You are advised to consult the publisher's version if you wish to cite this paper.

This version is being made available in accordance with publisher policies. See <http://orca.cf.ac.uk/policies.html> for usage policies. Copyright and moral rights for publications made available in ORCA are retained by the copyright holders.



Footwall degradation styles and associated sedimentary facies distribution in SE Crete: Insights into tilt-block extensional basins on continental margins

Tiago M. Alves¹, Tomas Cupkovic²

¹3D Seismic Lab, School of Earth and Ocean Sciences, Cardiff University, Main Building-Park
Place, CF10 3AT, Cardiff, United Kingdom

²Husky Energy, Atlantic Region, 351 Water St., Suite 105, St. John's, NL A1C 1C2, Canada

Abstract

Depositional facies resulting from footwall degradation in extensional basins of SE Crete are studied based on detailed geological maps, regional transects, lithological columns and outcrop photos. During an extensional episode affecting Crete in the late Miocene-early Pliocene, depocentres trending N20oE and N70oE were filled with fan deltas, submarine mass-wasting deposits, turbidites and fine-grained hemipelagites sourced from both nearby and distal sediment sources. Deposition of proximal continental and shallow-marine units, and relatively deep (marine) turbidites and mass-transport deposits, occurred within a complex mosaic of tectonically controlled depocentres. The new geological maps and transects in this work reveal that depositional facies in SE Crete were controlled by: a) their relative proximity to active faults and uplifting footwall blocks, b) the relative position (depth and relative height above sea level) of hanging-wall basins, and c) the nature of the basement units eroded from adjacent footwall blocks. Distal sediment sources supplied background siliciclastic sediment ('hemipelagites'), which differ markedly from strata sourced from local footwalls. In parallel, mass-transport of sediment was ubiquitous on tectonically active slopes, and so was the presence of coarse-grained sediment with sizes varying from large blocks >50 m-wide to heterolithic mass-transport deposits and silty-sandy turbidites. We expect similar tectono-

25 sedimentary settings to have predominated in tectonically active Miocene basins of the eastern
26 Mediterranean, in which hydrocarbon exploration is occurring at present, and on rifted continental
27 margins across the world.

28

29 **Keywords:** Extensional basins; Eastern Mediterranean Sea; Miocene; Messinian evaporites;
30 footwall degradation; depositional facies.

31

32 **1. Introduction**

33 Extensional (or syn-rift) basins are often filled by continental and shallow-marine deposits in their
34 initial stages, later forming marine depocentres as crustal stretching leads to fully rifted continental
35 margins (Mohriak and LeRoy, 2013; Ellis and Stoker, 2014; Leleu et al., 2016). Yet, their
36 depositional histories are still poorly documented in the literature, chiefly because syn-rift strata on
37 continental margins are frequently buried under thick post-rift successions. Extensional basins also
38 record complex (and markedly variable) evolutions depending on their position(s) relative to the
39 future axes of continental breakup (Nirrengarten et al., 2017; Alves and Cunha, 2018). A first
40 characteristic known to induce complexity in extensional systems is that proximal parts of future
41 continental margins become important sources of sediment to more distal rift axes, particularly as
42 the former are exhumed and become the shoulder areas of the latter during the last stages of rifting
43 and continental breakup (Braun and Beaumont, 1989; Huismans and Beaumont, 2011; Hartz et al.,
44 2017). Second, resulting continental-slope basins are predominantly filled by mass-wasting strata,
45 including disrupted channel-fill and turbidite deposits (so-called olistrostromes) whose development
46 and distribution are markedly controlled by the subsidence histories of discrete depocentres and
47 adjacent highs (Alves et al., 2009, Alves and Cunha, 2018). This characteristic often results in the
48 deposition of 'passive margin' olistrostromes containing both intraformational and exotic blocks
49 (Ogata et al., 2012; Festa et al., 2012, 2016), which are usually poorly imaged on seismic data (Liu

et al., 2016; Riedel et al., 2016). Third, the depositional architecture of syn-rift basins is also controlled by the nature of basement units, producing variable regoliths that are eroded at variable rates (and at different times) during crustal stretching (Blaich et al., 2011; Gerginon et al., 2014). This latter caveat is all the most important when considering that borehole data of syn-rift footwall degradation complexes are seldom documented in the literature.

In extensional basins, footwall degradation occurs not only on exposed (subaerial) tilt-blocks (Densmore et al., 2004, 2009), but also over submarine footwall blocks affected by strong currents and slope instability (Micallef and Mountjoy, 2011). Alternatively, thick salt and carbonate units may accumulate in closed, confined seas generated during continental breakup as documented, for instance, in SE Brazil and West Africa (Beglinger et al., 2012), or in the Central Atlantic Ocean (Tari and Jabour, 2013). Dominated either by evaporite, carbonate or siliciclastic deposition, hyperextended blocks close to the loci of continental breakup record enhanced faulting, footwall degradation and erosion (Alves et al., 2009; Jeanniot et al., 2016; Alves and Cunha, 2018).

As the few examples of marine syn-rift strata documented in the literature have focused on continental margins drilled by the Deep-Sea (DSDP), Ocean Drilling (ODP) and International Ocean Drilling (IODP) programmes, or used geophysical data of insufficient quality beyond a certain depth (e.g., Wilson et al., 2001; Tucholke and Sibuet, 2007), there is a pressing need in academia and industry for new outcrop analogues of extensional basins revealing structures and stratigraphic sequences of similar scales to those imaged on state-of-the-art seismic data. Southeast Crete is one such analogue region, and records the deposition of late Miocene strata sourced from nearby footwall blocks, continental shelves and distal slopes under significant late Miocene extension (Fortuin, 1978; Peters, 1985; Postma and Drinia, 1993; ten Veen and Postma, 1999; Alves et al., 2007; Alves and Lourenço, 2010) (Fig. 1).

A new set of depositional facies maps for SE Crete is presented here based on a reassessment of stratigraphic formations interpreted in Fortuin et al. (1977), Postma and Drinia (1993) and ten Veen

75 and Postma (1999). We reassessed the significance of distal marine strata outcropping on coastal
76 areas of SE Crete to understand the degree of stratigraphic overlap (i.e., lateral variations in facies)
77 between distal marine successions and more proximal strata in extensional basins (Fig. 1). In order
78 to achieve this goal, we grouped the regional tectono-stratigraphic units defined by Postma (1990)
79 and Postma and Drinia (1993) into genetic units, and analysed them in the context of a rifting, fault-
80 dominated, South Aegean region during the late Miocene. This study has implications for the
81 interpretation of: a) pre-evaporite successions in the Eastern Mediterranean Sea, and b) syn-rift
82 successions on deep-water continental margins.

83

84 **2. Materials and methods**

85

86 This work presents new geological maps, regional transects, lithological logs and outcrop photos
87 from SE Crete. It documents the basin expansion in the investigated area, where a series of hanging-
88 wall basins and adjacent footwall blocks are exposed (Figs. 1c, 2). The approach followed in this
89 study was to reassess morphological and sedimentological features related to (syn-rift) footwall
90 degradation as recorded by upper Miocene strata (Figs. 2a, 2b). In addition, we conducted a re-
91 mapping of the Fothia Formation (Fortuin, 1974) in the region east of the city of Ierapetra. The
92 sediments of Fothia Formation were re-interpreted as a lateral equivalent of strata spanning the
93 entire late Miocene in the Ierapetra Graben and surrounding paleoslopes (Fig. 2b).

94 Our geological data were acquired using army maps at a 1:50,000 scale (Hellenic Mapping and
95 Cadastral Organization) as reference maps. Relative ages for the interpreted stratigraphic formations
96 are based on Fortuin (1977, 1978); Meulenkamp (1979), Peters (1985), Postma and Drinia (1993),
97 Postma et al. (1993), Van Hinsbergen and Meulenkamp (2006) and Zachariasse et al. (2008). Most
98 of these ages derive from detailed micropaleontological analyses of foraminiferal assemblages

99 collected in the Ierapetra Graben (e.g., Fortuin, 1977; Fortuin and Peters, 1984; Peters, 1985;
100 Zachariasse et al., 2008).

101

102 **3. Geological Setting**

103

104 *3.1 Late Cenozoic convergence and extension in the Eastern Mediterranean*

105

106 The Eastern Mediterranean Sea, in which Crete is located, was first generated by the segmentation
107 of the Pangean supercontinent (Koukouvelas and Doutsos, 1990; Burg et al., 1996; Koukouvelas
108 and Aydin, 2002), and was deformed during the late Mesozoic-Cenozoic due to convergence
109 between the African, Eurasian and Arabic tectonic plates (Thomson et al., 1999; Romer et al., 2008)
110 (Fig. 1a). The closure of the Neotethys Ocean produced E-W structures in the Aegean region, which
111 accreted with a microcontinent (Apulia) to generate the Hellenic Arc and associated tectonic nappes
112 in the late Cretaceous-Paleogene (Stampfli, 2000). These nappes form the basement units of Greece
113 and surrounding islands (Kissel and Laj, 1988; Pearce et al., 2012; Sachpazi et al., 2016) (Fig. 1b).

114 The Hellenic Nappes comprise the dominant basement sequences of Crete, and two main units are
115 usually recognised in them; a pre-Neogene unit and a Neogene unit, the latter of which includes
116 strata accumulated in supradetachment basins (van Hinsbergen et al., 2006) (Figs. 1b, 2a). Thus,
117 Crete comprises a nappe of non-metamorphic rocks (Upper Sequence) over which Neogene strata
118 were deposited, and a metamorphic unit named the Lower Sequence (van Hinsbergen et al., 2006;
119 Kokinou et al., 2012) (Fig. 1b, 2a). Separating the Lower and Upper Sequences are several
120 extensional detachments of Oligocene-Miocene age that outcrop in parts of Crete (Figs. 1b, 2a).
121 These extensional detachments have exhumed the Lower Sequence over footwall blocks to form
122 extensional klippen on Crete, and several islands and offshore structural highs of the Aegean Sea.

123 Extensional detachments are chiefly located at the base of the Upper Sequence, i.e., close to the
124 contact with Cycladic Blueschists, granites and metamorphic basement rocks (Fig. 2a).

125 At present, the Aegean Sea records 90o convergence west of central Greece, with a change towards
126 an oblique configuration south of Crete (Papazachos et al., 2000; Bohnhoff et al., 2005; Shaw and
127 Jackson, 2010). This obliquity in the convergence vectors is responsible for important transtension
128 south of Crete, and has triggered a long period of extensional collapse since the Middle Miocene
129 (Fassoulas et al., 1994; Ring et al., 2001; Papanikolaou and Vassilakis, 2010) (Fig. 1a). Importantly,
130 sidescan sonar and high-resolution seismic data show, at present, a similar tectono-stratigraphic
131 setting to the late Miocene. Similar depositional facies to those exposed in the Ierapetra Graben
132 predominate along the modern continental slope of South Crete (Alves et al., 2007; Kokinou et al.,
133 2012).

134

135 *3.1.1 Lower Sequence*

136

137 The Lower Sequence includes a thick succession of phyllites, quartzites (Phyllite-Quartzite Unit)
138 and ‘paraautochthonous’ rocks in the Plattenkalk Series, a hard carbonate-rich series forming the
139 core of Crete’s mountains (Creutzburg et al., 1977; Thomson et al., 1999; Papanikolaou and
140 Vassilakis, 2010). Data in Thomson et al. (1999) indicate that the High Pressure-Low Temperature
141 (HP-LT) rocks of Crete were subducted between 36 and 29 Ma (latest Eocene-early Oligocene),
142 heated to peak temperatures in excess of 350°C, and then rapidly cooled to below 290°C prior to 19
143 Ma (Burdigalian). These same HP-LT rocks were at temperatures below 60°C at ~ 15 Ma
144 (Langhian). The Plattenkalk Series should have undergone the same sequence of events in an even
145 shorter time period, i.e., as short as 10 Ma (Thomson et al., 1999). Thus, depths of <10 km and
146 temperatures <300oC predominated after 19 Ma (Burdigalian) in what were, prior to their
147 exhumation, HP-LT units buried at depths of 30-40 km (Thomson et al., 1999).

148

149 3.1.2 *Upper Sequence and overlying supradetachment basins*

150

151 The Upper Sequence on Crete comprises non-metamorphic rocks and younger sediments (Ring et
152 al., 2001). In SE Crete, non-metamorphic Upper Cretaceous–Eocene rocks are part of the highly
153 faulted Tripolitza unit (Zambetakis-Lekas et al., 1998; Ring et al., 2001). Above these limestones
154 were deposited Neogene strata in supradetachment (extensional) basins (Ring et al., 2001) (Fig. 2b).
155 According to Meulenkamp et al. (1994), Langhian strata in the Mithi Formation (at the base of the
156 Miocene sequence in SE Crete) represent deposition in a fluvial peneplain and, therefore, can be
157 used as a marker of tectonic movements (subsidence and uplift) on the island.

158

159 3.2. *Facies associations in supradetachment basins*

160

161 Meulenkamp et al. (1979) divided the Neogene (supradetachment) units of Crete into six
162 stratigraphic groups; Prina, Tefeli, Vrisses, Hellenikon, Finikia, and Agia Galini (Alves et al., 2007,
163 their Fig. 2). Stratigraphically, these groups are observed below thin, undifferentiated Quaternary
164 strata. Locally in the Ierapetra Graben, Postma and Drinia (1993) subdivided the six stratigraphic
165 groups of Meulenkamp et al. (1979) in facies associations. These facies associations reflect
166 proximal (continental) to distal (marine) environments:

167 a) Facies associations A to C (Fa A-C) comprise deep-water delta and slope systems forming the
168 most part of the Kalamavka and Makrilia Formations (Figs. 2b, 3d, 4). Fa A comprises channel-fill
169 pebble to cobble conglomerates that are up to 2–3 m thick and massively bedded. They are included
170 in bioturbated laminated sand and mud intervals. Fa A is generally sandier and more stratified than

171 the conglomerates embedded in Fa B–C (Figs. 3d, 4). Facies associations B and C comprise finer-
172 grained material, mostly representing turbidite deposits, with distinct amounts of coarse-grained
173 material. In contrast to Fa B, the finer-grained Fa C shows rare sandstone intervals and is essentially
174 composed of blue-grey fossiliferous marls with abundant Zoophycos ichnofacies. Much of the
175 coarse-grained material in these deep-water systems suggests a slope environment where seafloor
176 instability was common and tectonic oversteepening prevailed. Postma and Drinia (1993) present
177 evidence for submarine slope channels incising into delta slopes, and transferring small lobe
178 deposits in the form of thin turbidites sandstone sub-units with sheet-like geometries. According to
179 the latter authors, such a character indicates a lateral shift in point sources of sediment.

180 b) Facies association 1, or Fa1, comprises alluvial systems and mass-flow deposits that alternate
181 with conglomerate beds deposited by cohesive debris flows, sensu Lowe (1982). This facies
182 association is chiefly represented by the Males Formation, but is also visible in parts of the Fothia
183 Formation on the eastern shoulder of the Ierapetra Graben (Figs. 1c, 2b, 3a). Stream-flow deposits
184 can be documented at Kalamavka and also east of Ierapetra (Fig. 1c). Current directions are
185 predominantly to the south and southwest (Alves and Lourenço, 2010) (Fig. 5).

186 c) Facies associations 2 to 4 (Fa 2-4) comprise delta and prodelta units. They were deposited by a
187 shallow-water delta system around Ierapetra and later disrupted on tectonically active slopes to
188 form the Prina Series (Postma and Drinia, 1993) (Figs. 2b, 3b, 3c). Typical lithologies in Fa 2-4 are
189 ungraded and graded pebbly sandstone beds, fine to coarse-grained sandstone sheets, and thin-
190 bedded sandstones and marls. Burrows are common in Fa 2-4 and include Skolithos, Chondrites
191 and Thalassinoides ispp. Boulder conglomerates comprise structureless lobe-shaped beds that are up
192 to 2 m thick. Intervals with sand and silt in Fa 2-4 were affected by wave action and likely triggered
193 by stream floods and hyperpycnal flows during periods of extreme water discharge.

194 In addition to facies associations of Postma and Drinia (1993), Postma et al. (1993) and ten Veen
195 and Postma (1999) interpreted five post-mid Miocene tectonic sequences on Crete (Table 1). We
196 acknowledge the latter tectonic sequences in this work, but we divide the strata observed in the field

197 into specific genetic units as we found strata on coastal outcrops to be less time-specific than
198 considered by Postma et al. (1993) and ten Veen and Postma (1999). Hence, the focus is given in
199 this work to depositional facies, not tectonic sequences, as seemingly synchronous strata present
200 distinct depositional facies along SE Crete, as also suggested by Fortuin (1977, 1978) (see regional
201 correlation panel in Fig. 2b, Table 1).

202

203 **4. Results**

204

205 *4.1 Key structures and lithologies at outcrop*

206

207 The new maps and corresponding transects in this paper reveal three distinct zones in SE Crete
208 (Figs. 6-8). The three zones follow, and are separated by, faults striking WNW (N70o E to N90oE)
209 and NE-SW (N20oE to N40oE).

210 Zone 1 stretches from Arvi to Gra-Ligia (Fig. 6). Here, a series of N70oE to N90oE faults bound a
211 late Serravalian-early Pliocene continental slope exhumed in the Quaternary to expose a series of
212 marine units (Fig. 4, Table 1). Zone 1 comprises autochthonous carbonate fans and boulder
213 conglomerates interbedded with slope turbidites (Figs. 6, 9). Turbidites and individual mass-
214 transport deposits are more abundant on coastal outcrops, reflecting a distal slope succession with
215 prominent gully and channel-fill deposits. Sand-mud ratios in this area are relatively high as
216 channels were capable of transferring coarse-grained material from hinterland sources (Figs. 6, 9,
217 10).

218 Inland, towards the village of Anatoli, there is a gradual increase in the volume of carbonate
219 megabreccias and fan-delta deposits (Fig. 7). In addition, most of the Males Formation is disrupted

220 and fragmented in discrete blocks. Boulder conglomerate units of Fa 2–4 predominate in proximal
 221 regions of Zone 1 (to the north), whereas Fa A to C are common on the coast, where a relatively
 222 deeper late Miocene-Pliocene depocentre was located (Figs. 7-12).

223 Zone 2 corresponds to the Ierapetra Graben, which is bounded by the Anatoli anticline (and
 224 associated paleoslope) to the northwest, and to the east by the southwards prolongation of the
 225 Ierapetra Fault to the south; the Ierapetra Cape Horst (Fig. 7). This horst is blanketed by a large,
 226 faulted mass-transport complex (Fothia Formation) that spans most of the late Miocene (Fig. 7). To
 227 the west of the Ierapetra Cape Horst, the Ierapetra Graben was filled by a minimum of 1400 m of
 228 sediments in the late Miocene-early Pliocene (Fortuin, 1977).

229 The Ierapetra Graben is bounded to the north by a series of faults marking the Makrilia Fault Zone
 230 sensu Postma and Drinia (1993). Zone 2 is dominated by distal marine facies (Fa A to C), deposited
 231 within the main basin depocentre in the SE Crete, the Ierapetra Graben (Figs. 7, 13, 14). The two
 232 shoulders of this graben record important mass-wasting with large scale megabreccia blocks
 233 dominating the successions deposited there (Figs. 13, 14). In these two shoulder areas, boulder-
 234 conglomerate and megabreccia blocks overlie continental to shallow-marine siliciclastic units of the
 235 Males Formation (Figs. 2b, 14). This setting is well documented on the western shoulder of the
 236 Ierapetra Graben, whereas a combination of fault scarps and displaced megabreccia blocks is
 237 observed towards the east at Fothia (Fig. 13). The same region documents the intersection of ENE-
 238 WSW and NNE-SSW faults and comprises large slide blocks embedded in marine (Makrilia
 239 Formation equivalent) siliciclastic sediments (Fig. 11).

240 Zone 3 includes the region east of Ierapetra, from Ferma to Makri Gialos, and includes the southern
 241 prolongation of a sedimentary basin named as Sitia Basin by ten Veen and Postma (1999) (Fig. 8).
 242 In this region, a series of tilt-blocks and associated half-graben basins (generally trending N70oE to
 243 N90oE) are filled with continental/alluvial to deep-marine strata, as shown later in this paper. Zone
 244 3 comprises alluvial fan deltas vertically stacked in between ‘background’ shelf sandstones and

245 mudstones with a characteristic yellow to white colour (Figs. 15, 16). In places, strata in alluvial
246 cones and fan deltas dip towards the North due to local rotation of tilted blocks (Fig. 17a). South of
247 the area of tilt-block rotation is observed a marked change in facies towards Fa A to C, which
248 predominate in coastal outcrops (Fig. 17b). Structural deformation at some of these coastal outcrops
249 is clearly associated with local extensional faults, tilt-block rotation, and with prominent (slope)
250 instability of marine successions of Fa A to C (Fig. 17b, 17c).

251

252 4.2 Genetic units associated with footwall degradation

253

254 In this work, we reassess the facies associations documented in Postma and Drinia (1993) in larger
255 genetic units that are specifically associated with footwall degradation, and correlate to seismically
256 resolvable units on geophysical data.

257

258 4.2.1 Fan deltas

259

260 Description: Fan deltas (Fa1) are observed in the northernmost parts of Zones 1 and 3 as the most
261 proximal deposits in SE Crete (Figs. 6-8). Fan deltas are chiefly observed on the paleoslopes
262 bordering the Ierapetra Graben, where they comprise autochthonous megabreccia fans and rotated
263 slabs tens to hundreds of metres thick (Fig. 14). In Zone 3, fan deltas are fed from distinct basement
264 units, and include polymictic breccias and conglomerates. These fan deltas are stacked vertically on
265 top of rotated hanging-wall blocks (Figs. 18, 19). Clasts in these polymictic breccias were derived
266 from Tripolitza and flysch units that outcrop in nearby mountains. In addition, dispersed clasts of

267 higher-grade metamorphic rocks include marbles and ophiolites sourced from rocks below the
268 Cretan detachment (i.e., Lower Sequence) (Fig. 3d).

269 One such example is observed east of Kalamavka village, where alluvial systems of facies
270 association 1 (Fa1) are abundant within the Males Formation (Figs. 2b, 3c). A second example is
271 recorded at Agios Ioannis (Fig. 19). Here, limestone rich fan deltas breccia–conglomerates were
272 deposited above shallow marine strata equivalent to the shallower part of Kalamavka Formation
273 (Fig. 2b). Isolated disrupted sediment blocks that are not part of the Prina series rest above (or are
274 partly embedded within) marine clays, marls, and sands belonging to facies associations similar to
275 those in the Kalamavka Formation (Fig. 2b, 19).

276 Breccia–conglomerate fans are mainly documented in Zone 3, where stacked successions of fan
277 deposits occur over rotated half-grabens (Figs. 8, 17). Here, breccia–conglomerates show a
278 predominance of carbonate clasts derived from Tripolitza and Plattenkalk basement units, but also
279 mixed with higher grade metamorphic clasts derived from the Flysch unit and from units below the
280 Cretan detachment.

281

282 Interpretation: Fan deltas in SE Crete are dominated by mass-flow deposits, with conglomerate beds
283 originating from cohesive debris flows, sensu Lowe (1982), whereas stream-flow deposits are
284 observed around the village of Kalamavka (Fig. 7). Current directions in these latter alluvial
285 systems are predominantly to the S and SE as revealed by cross-bedding geometries, imbricated
286 clasts and lateral facies variations within the Males Formation (Figs. 2b, 5).

287 Vertical stacking of fan deltas was an important process in proximal parts of Zone 3, with E-W half-
288 graben basins becoming the location of significant breccia-conglomerate deposition (Figs. 14, 18).
289 Fan deltas were fed by alluvial fans, are smaller than the deltas of contemporary rivers, and are
290 characterised by large variations in morphology, geometry and facies (Postma, 1990). Therefore,
291 the prominent structural style in this type of deposits is one controlled by active normal faults that

292 dissect the slope, oversteepening and fracturing the basement to develop footwall degradation
293 products. This is particular the case for Zone 3, whereas fan deltas in Zone 1 contain less angular
294 breccia-conglomerates, which indicate relatively longer sediment transport.

295

296 4.2 Mass-transport deposits and oversteepened (slumped) strata

297

298 Description: Mass-transport deposits (Fa2-4 and A-C) are abundant in Zones 1 and 3, and often
299 occur together with large 5–100 m-wide blocks in distal parts of fan deltas in Fa 2-4 (Figs. 3a, 19).
300 These blocks were separated from fan deltas during late Miocene tectonics and were mostly
301 transported downslope over a ductile substrate (see Alves and Lourenço, 2010). Towards the
302 easternmost part of Zone 1, large blocks give rise to discrete mass-transport deposits and slabs,
303 most of which remobilised carbonate and sandy intervals in lower-slope stratigraphic successions.
304 Thus, there is an overall tendency for slumped strata and discrete (but relatively thin) mass-
305 transport deposits to occur at coastal outcrops in Zone 1, with sporadic blocks being observed here
306 (Fig. 6). In turn, the more proximal parts of the paleoslope in Zone 1 reveal the presence of large
307 slide blocks that are buttressed against slope strata of Makrilia and Ammoudhares facies (Figs. 3a,
308 6).

309 An example of the importance of mass-transport to the development of palaeoslopes in Zone 3 is
310 shown west of Makri Gialos where slumps occur over a wide area (Fig. 8). Here, intraformational
311 slumps can form thick successions of disrupted strata that not only contain ‘background’
312 siliciclastic material, but also slumped channel-fill deposits, limestone and sandstone blocks
313 disrupted on a tectonically active slope (Fig. 19).

314

315 Interpretation: These deposits are typical of a slope environment where rivers and streams are
316 capable of bypassing the narrow continental shelf to form submarine channels on the slope. Most
317 channel-fill sediments show some degree of tectonic oversteepening and later collapse on marine
318 slopes (Figs. 8, 19). The Ammoudhares Formation caps these channel-fill strata and comprises
319 marls and bioclastic limestones reflecting a relative shallowing of the region during the Messinian
320 (Fig. 2b).

321 Large slumped masses of calcarenites and turbidites devoid of slide blocks are indicative of slope
322 oversteepening on local paleoslopes. This character is commonly observed within the Makrilia and
323 Ammoudhares formations, with slumped strata being scattered on coastal outcrops that extend from
324 the village of Ammoudhares to Arvi, both in Zone 1 (see Fig. 10 as example). In these areas,
325 slumping occurred in intervals with sandy interbedded channel-fill deposits and (finer-grained)
326 hemipelagites. Slumping can be local (affecting a few metres of strata) to involving large slabs 50-
327 100 m in length. In Zone 3, the mud-rich matrix in boulder conglomerates suggests deposition from
328 cohesive debris flows, in a setting dominated by slope instability and block movement over a
329 ductile, oversteepened slope. Reservoir potential is relatively poor in these gravitational units as
330 sands composing discrete clasts have been cemented prior to mass-wasting. Carbonate blocks also
331 have a clayey matrix that derives from deposition in proximal alluvial fans prior to their disruption
332 on the continental slope (Alves and Lourenço, 2010).

333

334 4.3 Undisturbed (background) hemipelagites

335

336 Description: Background hemipelagites and distal submarine fan deposits are particularly observed
337 in the Myrtos area, in the Ierapetra Graben, and at Cape Ierapetra (Figs. 6-8, 16). They comprise
338 loosely consolidated silty sands and clays interbedded with channel-fill deposits comprising a >
339 1000 m-thick succession at Makrilia, and approximately 500 m-thick at Myrtos (Fig. 8). Turbidite

340 deposits are mostly fine-grained at the limit between Zones 2 and 3 (Fig. 7). Distal submarine fan
341 deposits are not observed in Zone 3, around Makri Gialos. Instead, a series of shelve deposits with
342 important carbonate contribution is recorded by the deposition of sand-silty successions with
343 coarser channel and submarine-fan deposits (Fig. 8).

344

345 Interpretation: The relative scarcity of sand in Zone 2 indicates that the area was relatively far from
346 local sediment sources. These sediments are, towards the east in Zone 3, increasingly interbedded
347 with channel-fill breccias and conglomerates representing episodes of channel erosion derived from
348 footwall blocks to the north.

349 Slope turbidites are abundant in Zone 1, in proximal parts of Zone 2, but occur only at coastal
350 outcrops in Zone 3 (Fig. 8). Background sediment comprises silt and clay with variable amounts of
351 dispersed sand - often resting on south-facing monoclines (Figs. 17, 18). In Zone 1, strata in the
352 Makrilia and Ammoudhars formations are deformed ahead of a large recumbent fold, and show
353 remobilised channel overbank sands and silts in coastal outcrops (Alves and Lourenço, 2010, their
354 Fig. 14). Fracturing and injection of sandy layers associated with this frontal fold denotes a ductile
355 regime occurring typically a few metres below the paleoseafloor.

356

357 4.4 Gully- and channel-fill deposits

358

359 Description: Gully and channel-fill deposits are ubiquitous at coastal outcrops of Zones 1 and 3, and
360 in several locations around the village of Makrilia (Zone 2) (Fig. 7). This type of deposit comprises
361 polymictic breccias and conglomerates that were chiefly sourced from basement units. Grain size
362 varies from well sorted coarse- to medium-sands, to polymictic gravel and conglomerate channel-
363 fill deposits (Fig. 17). Limestone clasts and boulders are prominent in most coarse-grained deposits.

364 Gully and channel-fill deposits are also exposed in Zone 3 around Agios Ioannis, occupying similar
365 space as modern subaerial gorges (Fig. 18). This indicates a structural control on the position and
366 distribution of channels, gullies and gorges in the SE Crete. In Zone 1, channel-fill deposits are part
367 of the oversteepened slopes element.

368 Channel-fill deposits in Zone 2 are observed around the village of Makrilia, where they incise
369 background silts and clays. Their origin is marine, and they reflect episodic erosion of the Makrilia
370 paleohigh, which was providing most of the feeding material to the north in the form of fan deltas
371 and prodelta deposits, some of which resembling breccia-conglomerates in the Prina Group (Figs.
372 2b, 3a, Table 1).

373 Zone 3 records the incision of channels and gullies in specific areas of the late Miocene paleoslope,
374 and likely involved an underlying fault-related structural control. Between Agios Ioannis-
375 Sinokapsala, channel-fill deposits are composed of coarse sand and gravel showing massive
376 bedding (Figs. 18, 19). They are intercalated with shelval deposits into which they were incising,
377 and with intervals containing blocks and megabreccias. In this same Zone 3, breccia-conglomerates
378 are markedly coarse, involving the deposition of boulders and large blocks in the fan deltas
379 themselves (Fig. 19). Fan delta sediment becomes relatively finer (but still comprising breccia-
380 conglomerates) in the southernmost tips of fan deltas, suggesting they were deposited in subsiding
381 half-grabens roughly oriented E-W (Fig. 8).

382

383 Interpretation: The interpreted depositional systems reflect the incision of channels during relative
384 lowstands (or episodes of footwall uplift), with NE-SW faults leading to the formation of relays
385 between developed N70oE-N90oE faults. These faults and relay zones provided preferential
386 pathways for transport and deposition of products of footwall degradation in the form of streams,
387 channels and fan deltas developed on the paleoshelf, whereas continuous fault strands fed large

388 slide blocks and megabreccias towards evolving depocentres. Such a character indicates that
389 turbidite and mass-transport deposition were occurring at the same time and where complementary.

390 In Zones 1 and 2, channel-fill deposits alternate with sandstones and conglomerates in main basin
391 depocentres, and with coarsening-upwards massive/parallel-laminated red marls and clays. Finning-
392 upwards turbidites are related to deposition on a fault-bounded slope. Sequences Ta, Tbe/Tbde and
393 Tbcde of Bouma (1962) compose the bulk of the sandy deposits, but proximal Ta sequences
394 predominate in the coarser levels. Polymictic conglomerates and sands relate to submarine canyon
395 deposits. Massive marls, siltstones/sandstones and massive mudstones comprise, respectively,
396 lower-slope Td and Tet turbidites and distal Tet/Teh turbidites/hemipelagic fall-out.

397 Late Miocene-early Pliocene tectonics (i.e., prior to onset of uplift on Crete) is thus expressed by
398 the deposition of coarse-grained gully- and channel-fill units in the Makrilia and Ammoudhars
399 formations (Table 1). In a region extending from Tertsa to Arvi, marine channel-fill deposits
400 alternate with gravel fills that hint at more proximal, subaerial sources (Figs. 6, 19). We interpret
401 these latter channels as reflecting Quaternary tectonic uplift on Crete and, as such, they likely
402 reflect the erosion of renewed sediment sources. Most of these channel-fill deposits show a clear
403 fining-upwards trend in individual beds, which are stacked in discrete (>30) cycles of sand and silt
404 (Figs. 6, 10). Not every channel incises background slope deposits, with some seemingly emplaced
405 in slope depressions. In this case, overbank deposits show continuity towards the axis of channel-
406 fill strata, pinching-out gradually away from the same channel axes.

407

408 **6. Discussion**

409

410 *6.1 Local controls of basement lithology on footwall-degradation products*

411

412 A first question deriving from this study is why there is a significant presence of siliciclastic
413 deposits in the Ierapetra Basin and coastal outcrops of SE Crete when basement units of the whole
414 region are predominantly composed of carbonate rocks. One way to explain this discrepancy is by
415 considering the Ierapetra Basin and adjacent slope depocentres as part of a tectonically active,
416 collapsing Aegean microplate, whose morphology was distinct from the present day's
417 (Meleunkamp et al., 1994; ten Veen et al., 1999; Ring et al., 2001). In other words, the presence of
418 Miocene landmasses and erodible structural blocks close to the island of Crete explains, in the study
419 area, the large volume of siliciclastic units not related to eroded basement units.

420 It is widely known that a consequence of enhanced footwall degradation, either in continental or
421 marine extensional basins, is a relatively increase in the frequency (and thickness) of coarse-grained
422 material deposited adjacently to active structures (Gawthorpe and Leeder, 2000; Leeder et al., 2002).
423 In extensional basins dominated by siliciclastic depositional systems, the nature and grain size of
424 sediment are closely controlled by the nature of eroded 'basement' rocks (Leeder et al., 2002).
425 Basement rocks that are intrinsically brittle and fine-grained are more likely to produce clays, silts
426 and minor volumes of sand. Basement units dominated by granites and crystalline metamorphic
427 rocks will preferentially produce conglomerates, gravels and sands as predominant lithologies
428 (Knudsen, 2001; Lundmark et al., 2014). When capped by carbonates, subaerial karsts can develop
429 in exposed footwalls (Scheibner et al., 2003; Bosence, 2005; Tomás et al., 2010), whereas large
430 mass-wasting complexes often accompany the degradation of carbonate platforms to increase the
431 extent of reservoir units in immediate hanging-wall basins (Wilson et al., 2000; Bosence, 2005).
432 Farther offshore, carbonate platforms give rise to deep-marine shales and finer-grained material
433 (e.g., Loucks and Ruppel, 2006).

434 A second, but not less important, question concerns the reservoir potential of fan deltas, which are
435 clearly poorly graded and immature in their nature. Fan deltas in SE Crete occur on hanging-wall
436 depocentres that were formed very close to basement highs, a character implying very little
437 transport of sediment from immediate footwalls and fault scarps. In most of the area around Agios

438 Ioannis (Zone 3), the fan deltas comprise low porosity immature breccia-conglomerates, occurring
439 together with channelled bodies comprised of coarse sand and gravel. We interpret the breccia-
440 conglomerates as being directly derived from footwall scarps, whereas the channelled bodies were
441 fed by rivers and ephemeral streams capable of bypassing the fan deltas to input sediment in distal
442 slope depocentres (Figs. 14-19). In comparison, Zone 1 fan deltas at NW of Ierapetra are much
443 thinner, smaller in area and widespread laterally. They are also more mature in terms of the clasts
444 they contain, presenting conglomerates, gravel, sand and silt. This difference between fan deltas in
445 Zones 1 and 3 demonstrates a contrast in the lithology of basement units being eroded and relative
446 degree of uplift (i.e., fault activity) experienced by the eroded footwall blocks. Zone 1 fan deltas
447 were deposited on an immediate hanging-wall depocentres to the Ierapetra and Makrilia Faults and,
448 as such, represent a depositional setting of important sediment progradation from structural highs in
449 Zone 2 (Fig. 7). In contrast, Zone 3 fan deltas reflect important activity of N70oE faults and the
450 deposition of coarse-grained sediment in adjacent half-grabens (Fig. 8). In this area, footwall blocks
451 comprise Tripolitza and Plattenkalk limestones that were degraded and eroded to form very
452 immature fan deltas. We therefore postulate that the late Miocene-early Pliocene depositional facies
453 in SE Crete are structurally controlled, with terraced sets of half-grabens controlling the type and
454 thickness of sediment accumulated (Fig. 20).

455

456 6.2. Genetic units associated with continental slope basins: comparing SE Crete with drilled deep- 457 water continental margins

458

459 Figure 20 presents a schematic illustration (and corresponding lithological logs) across Zones 1 and
460 2 to illustrate the distribution of late Miocene-early Pliocene strata in SE Crete. In the study area,
461 we observe a tripartite distribution of sediment, with proximal, intermediate and distal depocentres
462 recording different facies associations. The very proximal depocentres formed at this time in

463 subsiding half-graben are filled with alluvial fans and fluvial deposits, which were affected by
464 important erosion and incision by Pliocene-Holocene streams formed due to tectonic uplift and fault
465 reactivation (Fig. 20). These proximal depocentres give rise to an intermediate area with transitional
466 and shallow-marine strata, effectively recording the late Miocene paleo-continental shelf. This shelf
467 was similar to the present-day's, being narrow and abruptly changing into a fault-bounded
468 continental slope towards the south. Slope deposits thus occur in a third set of half-graben basins in
469 the form of prograding sets of strata dominated by significant mass-wasting deposits (Fig. 20). In
470 such a setting, mass-wasting resulted from a combination of tectonic oversteepening of the paleo-
471 continental slope, high to very-high sedimentation rates during hyperpycnal and turbidite flows, and
472 control of sediment transport through submarine channels and gullies (Fig. 20).

473 Hence, the final question posed in this discussion is if deep-water margins across the world can
474 record similar depositional patterns to SE Crete. In the Antalya Basin of south Turkey, Miocene
475 compression deposited coarse grained fan deltas and fluvial deposits that appear to continue south
476 into contiguous offshore Miocene depocentres (Hall et al., 2014). Large, regional thrusts associated
477 with counter-clockwise rotation of the western side of the Isparta Angle (south Turkey) resulted in
478 the erosion of basement units to generate facies associations that are similar to those on Crete (e.g.,
479 upper Karpuzçay Formation and overlying Aksuçay and Köprüçay conglomerates; Çiner et al.,
480 2008). Cyprus records a similar late Miocene of siliciclastic influx into the region occurring in
481 response to the generation of a mosaic of carbonate platforms and interconnecting seaways in the
482 eastern Mediterranean region. This mosaic of basins was formed regardless if the predominant
483 tectonic regime was extensional, compressional or strike-slip (Eaton and Robertson, 1993;
484 Robertson, 2000; Schildgen et al., 2012). In the Aegean part of western Turkey, extension forces
485 predominated from the Middle Miocene, as on the island of Crete, leading to the coeval deposition
486 of footwall-degradation products in multiple E-W to WSW-ENE tectonic troughs (Angelier et al.,
487 1981; Seyitoğlu and Scott, 1991; Genç et al., 2001; Ocakoğlu et al., 2005).

488 In west Iberia, DSDP and ODP wells have drilled thick syn-rift siliciclastic units where the bulk of
489 the continental slope is carbonate in nature, with early-Mid Jurassic units comprising >3000 m of
490 carbonates in places (Boillot et al., 1987). On seismic data from west Iberia, syn-rift turbidites
491 alternate with mass wasting deposits that are, themselves, coarse grained and siliciclastic. The
492 break-up sequence is much finer grained, but mass transport deposits are still abundant within a
493 setting of forced regression on the continental shelf (Alves and Cunha, 2018). Offshore
494 Newfoundland, west Iberia and west Africa, the advanced rifting stages preceding continental
495 break-up denote the influx of siliciclastic material onto the future continental slope (Soares et al.,
496 2012; Beglinger et al., 2012). Sediment maturity in these regions depends, in theory, on
497 transporting distances from source areas and on the nature of basement units eroded on the margin,
498 apart from base level.

499 In summary, more than 1400 m of siliciclastic sediments deposited in the Ierapetra Graben during
500 late Miocene implies very high sedimentation rates in a setting recording the input of sediment from
501 large hinterland areas located in the Aegean Sea. The relative position of hinterland regions at that
502 time likely relate to a narrower Aegean in the late Miocene-early Pliocene, i.e., parts of continental
503 Greece and Turkey coasts were relatively close to Crete, with much larger numbers of structural
504 highs, islands and erodible footwalls in the Aegean Sea. We favour a tectono-sedimentary setting in
505 which extensional collapse in the Aegean Sea predominated during the late Cenozoic, with
506 subsequent formation of multiple sub-basins in around Crete. In a second stage, tectonic uplift of
507 the island during the Quaternary isolated the Cretan Trough from the extensional basins to the south
508 of the island (Alves et al., 2007; Kokinou et al., 2009).

509

510 **7. Conclusions**

511

512 Depositional styles of the sedimentary facies patterns of late Cenozoic strata in SE Crete are
513 displaying great variability both in the form of lithological composition and spatial distribution.
514 This characteristic of strata accumulated in the Ierapetra Graben, and exposed in numerous coastal
515 outcrops, is mostly a result of intense tectonic activity. A complex pattern of relatively uplifted and
516 subsiding blocks was produced in such extensional setting. The main results of this study can be
517 summarised as follows:

518

519 1. The highly faulted, brittle Tripolitza limestone unit fed a series of fan deltas, marine mass
520 wasting deposits and turbidites to late Cenozoic extensional basins on SE Crete. A series of basins
521 trending N20oE to N70oE-90o were filled by continental and transitional siliciclastic and carbonate
522 units (fan deltas) in proximal areas, whereas a complex fault bounded series of continental slope
523 basins were predominantly filled by turbidites and hemipelagic units.

524

525 2. Depositional facies in SE Crete were controlled by the relative depth of eroded footwall blocks,
526 the lithology and degree of structural disturbance of basement units, and paleo relief at the time of
527 deposition. Active normal faulting contributed for frequent oversteepening (and slumping) of strata
528 on the paleocontinental slopes bordering Crete. Rapid tectonic uplift and base level variations led to
529 the incision of submarine channels in specific parts of the paleoslope.

530

531 3. Mass wasting was ubiquitous in such a tectonically driven environment and, as a result, coarse
532 grained sediment varying in size from large blocks >50 m wide to silty-sandy calcarenites are
533 frequently observed in outcrop.

534

535 4. In the study area, genetic units with potential to form good quality reservoirs comprise: a) gully
536 and channel fill conglomerates and sandstones, and b) sand rich open slope turbidites and proximal
537 fan deltas. The relative porosity and sorting of sediment in these two genetic units show great
538 variability depending on their distance to main sediment source areas. These sediment source areas
539 are controlled by active faulting exposing basement units and older sediment to erosion.

540

541 5. In such a setting, open slope turbidites (when sand rich), represent the genetic unit with the
542 greatest potential to comprise volumetrically important reservoirs. Their geneses, distribution
543 patterns and relative ages are still to be understood, and need to be further correlated with other
544 Neogene basins on Crete, and within the wider context of late Miocene regional tectonics and
545 overriding regional sea level variations in the Mediterranean Basin. In addition, SE Crete provides
546 an important analogue to marine extensional basins on rifted continental margins that should be
547 compared and contrasted with other parts of the world in terms of reservoir character and potential.

548

549 **Acknowledgements**

550 This work was developed under research grants from the Royal Society, TEPA-Total Angola and
551 Husky Energy. The Geological and Mining Institute (IGME) in Greece is acknowledged for the
552 fieldwork permission awarded to both T. Alves and T. Cupkovic. The COST Action ES1301:
553 FLOWS - Impact of Fluid circulation in old oceanic Lithosphere on the seismicity of transfOrm-
554 type plate boundaries: neW solutions for early seismic monitoring of major European Seismogenic
555 zones in acknowledged for a meeting and field trip in 2016. We thank editor-in-chief J. Knight and
556 reviewer K. Ogata for their constructive comments.

557

558 **References**

559 Alves, T.M., Lykousis, V., Sakellariou, D., Alexandri, S., Nomikou, P., 2007. Constraining the
 560 origin and evolution of confined turbidite systems: southern Cretan margin, Eastern Mediterranean
 561 Sea (34°30–36°N). *Geo-Marine Letters* 27, 41-61.

562 Alves, T.M., Moita, C., Cunha, T., Ulnaess, M., Myklebust, R., Monteiro, J.H., Manuppella, G.,
 563 2009. Diachronous evolution of Late Jurassic-Cretaceous continental rifting in the northeast
 564 Atlantic (west Iberian margin). *Tectonics* 28, TC4003, doi:10.1029/2008TC002337.

565 Alves, T.M., Lourenço, S.D.N., 2010. Geomorphologic features related to gravitational collapse:
 566 Submarine landsliding to lateral spreading on a late Miocene–Quaternary slope (SE Crete, eastern
 567 Mediterranean). *Geomorphology* 123, 13-33.

568 Alves, T.M., Cunha, T.A., 2018. A phase of transient subsidence, sediment bypass and deposition
 569 of regressive–transgressive cycles during the breakup of Iberia and Newfoundland. *Earth and*
 570 *Planetary Science Letters* 484, 168-183.

571 Angelier, J., Dumont, J.F., Karamanderesi, H., Pissin, A., Şimşek, Ş., Uysal, Ş., 1981. Analyses of
 572 fault mechanisms and expansion of southwestern Anatolia since the late Miocene. *Tectonophysics*
 573 75, Issues 3-4, pages T1-T9, [https://doi.org/10.1016/0040-1951\(81\)90271-7](https://doi.org/10.1016/0040-1951(81)90271-7).

574 Beglinger, S.E., Doust, H., Cloething, S., 2012. Relating petroleum system and play development to
 575 basin evolution: Brazilian South Atlantic margin. *Petroleum Geoscience* 18, 315-336.

576 Blaich, O.A., Faleide, J.I., Tsikalas, F., 2011. Crustal breakup and continent-ocean transition at
 577 South Atlantic conjugate margins. *Journal of Geophysical Research: Solid Earth* 116, B01402,
 578 doi:10.1029/2010JB007686.

579 Bohnhoff, M., Harjes, H.-P., Meier, Th., 2005. Deformation and stress regimes in the hellenic
 580 subduction zone from focal mechanisms. *Journal of Seismology* 9, 341-366.

581 Boillot, G., Winterer, E.L., Meyer, A.W., et al., 1987. Proc. ODP, Init. Repts., 103, College Station,
582 TX (Ocean Drilling Program). doi:10.2973/odp.proc.ir.103.1987.

583 Bosence, D., 2005. A genetic classification of carbonate platforms based on their basinal and
584 tectonic settings in the Cenozoic. *Sedimentary Geology* 175, 49-72.

585 Bouma, A.H., 1962. *Sedimentology of some Flysch deposits: A graphic approach to facies*
586 interpretation. Elsevier, Amsterdam, 168

587 Braun, J., Beaumont, C.A., 1989. Physical explanation of the relation between flank uplifts and the
588 breakup unconformity at rifted continental margins. *Geology* 17, 760-764.

589 Buckley, J.P., Bosence, D., Elders, C., 2015. Tectonic setting and stratigraphic architecture of an
590 Early Cretaceous lacustrine carbonate platform, Sugar Loaf High, Santos Basin, Brazil. In: Bosence,
591 D.W.J., Gibbons, K.A., Le Heron, D.P., Morgan, W.A., Pritchard, T., Vining, B.A. (Eds), *Microbial*
592 *Carbonates in Space and Time: Implications for Global Exploration and Production Geological*
593 *Society of London, Special Publications* 418, 175-191. Burg, J.P., Ricou, L.E., Ivano, Z., Godfriaux,
594 I., Dimov, D., Klain, L., 1996. Syn-metamorphic nappe complex in the Rhodope Massif: Structures
595 and kinematics, *Terra Nova* 8, 6–15.

596 Çiner, A., Karabiyikoğlu, M., Monud, O., Deynouz, M., Tuzcu, S., 2008. Late Cenozoic
597 Sedimentary Evolution of the Antalya Basin, Southern Turkey. *Turkish Journal of Earth Sciences*
598 17, 1-41.

599 Creutzburg N., Drooger, C.W., Meulenkamp, J.E., Papastamatiou, J., Seidel, E., Tataris, A., 1977.
600 Geological map of Crete (1:200.000). Institute of Geology and Mineral Exploration (IGME).
601 Division of general geology and economic geology.

602 Densmore, A.L., Dawers, N.H., Gupta, S., Guidon, R., Goldin, T., 2004. Footwall topographic
603 development during continental extension. *Journal of Geophysical Research. Earth Surface* 109,
604 F03001, doi:10.1029/2003JF000115.

605 Densmore, A.L., Hetzel, R., Ivy-Ochs, S., Krugh, W.C., Dawers, N., Kubik, P., 2009. Spatial
606 variations in catchment-averaged denudation rates from normal fault footwalls. *Geology* 37, 1139-
607 1142.

608 Eaton, S., Robertson, A., 1993. The Miocene Pakhna Formation, southern Cyprus and its
609 relationship to the Neogene tectonic evolution of the Eastern Mediterranean. *Sedimentary Geology*
610 86, 273-296.

611 Ellis, D., Stoker, M.S., 2014. The Faroe–Shetland Basin: a regional perspective from the Paleocene
612 to the present day and its relationship to the opening of the North Atlantic Ocean. In: Mohriak,
613 W.U., Danforth, A., Post, P.J., Brown, D.E., Tari, G.C., Nemčok, M. and Sinha, S.T. (Eds.),
614 *Conjugate Divergent Margins: Geological Society, London, Special Publications* 397, 497-535.

615 Festa, A., Dilek, Y., Pini, G.A., Codegone, G., Ogata, K., 2012. Mechanisms and processes of
616 stratal disruption and mixing in the development of mélanges and broken formations: Redefining
617 and classifying mélanges. *Tectonophysics* 598, 7-24.

618 Festa, A., Ogata, K., Pini, G.A., Dilek, Y., Alonso, J.L., 2016. Origin and significance of
619 olistostromes in the evolution of orogenic belts: A global synthesis. *Gondwana Research* 39, 180-
620 203.

621 Fortuin, A.R., 1977. Stratigraphy and sedimentary history of the Neogene deposits in the Ierapetra
622 region, eastern Crete. Doctoral Thesis, University of Utrecht, 1977, GUA Papers of Geology Ser. 1,
623 No 8, 164pp.

624 Fortuin, A.R., 1978. Late Cenozoic history of Eastern Crete and implications for the geology and
625 dynamics of the Southern Aegean Area. *Geologie en Mijnbouw* 57, 461–464.

626 Fortuin, A.R., Peters, J.M., 1984. The Prina Complex in eastern Crete and its relationship to
627 possible Miocene strike-slip tectonics. *Journal of Structural Geology* 6, 459–476.

628 Gawthorpe, R.L., Leeder, M.R., 2000. Tectono-sedimentary evolution of active extensional basins.
629 Basin Research 12, 195-218.

630 Gernigon, L., Brönnert, M., Roberts, D., Olesen, O., Nasuti, A., Yamasaki, T., 2011. Crustal and
631 basin evolution of the southwestern Barents Sea: From Caledonian orogeny to continental breakup.
632 Tectonics 33, 347–373.

633 Hall, J., Aksu, A.E., King, H., Gogacz, A., Yaltirak, C., Çifçi, G., 2014. Miocene–Recent evolution
634 of the western Antalya Basin and its linkage with the Isparta Angle, eastern Mediterranean. Marine
635 Geology 349, 1-23.

636 Hartz, E.H., Medvedev, S., Schmid, D.W., 2017. Development of sedimentary basins: differential
637 stretching, phase transitions, shear heating and tectonic pressure. Basin Research 29, 591–604..

638 Huismans, R., Beaumont, Ch., 2011. Depth-dependent extension, two-stage breakup and cratonic
639 underplating at rifted margins. Nature 473, 74-78.

640 Jeannot, L., Kuszniir, N., Mohn, G., Manatschal, G., Cowie, L., 2016. Constraining lithosphere
641 deformation modes during continental breakup for the Iberia–Newfoundland conjugate rifted
642 margins. Tectonophysics 680, 28-49.

643 Kissel, C., Laj, C., 1988. The Tertiary geodynamical evolution of the Aegean Arc, a paleomagnetic
644 reconstruction. Tectonophysics 146, 183–201.

645 Knudsen, T.-L., Fossen, H., 2001. The late Jurassic Biorøy Formation: A provenance indicator for
646 offshore sediments derived from SW Norway as based on single zircon (SIMS) data. Norsk
647 Geologisk Tidsskrift 81, 283-292.

648 Kokinou, E., Alves, T., Kamberis, E., 2012. Structural decoupling in a convergent forearc setting
649 (southern Crete, Eastern Mediterranean). Bulletin of the Geological Society of America 124, 1352-
650 1364.

651 Koukouvelas, I., Aydin, A., 2002. Fault structure and related basins of the North Aegean Sea and its
652 surroundings. *Tectonics* 21, Issue 5, 1–17.

653 Koukouvelas, I., Doutsos, T., 1990. Tectonic stages along a traverse cross cutting the Rhodopian
654 zone (Greece). *Geologische Rundschau* 79 (3), 753–776.

655 Leeder, M., Collier, R., Abdul Aziz, L., Trout, M., Ferentinos, G., Papatheodorou, G., Lyberis, E.,
656 2002. Tectono-sedimentary processes along an active marine/lacustrine half-graben margin:
657 Alkyonides Gulf, E. Gulf of Corinth, Greece. *Basin Research* 14, 25-41.

658 Leleu, S., Hartley, A.J., van Oosterhout, C., Kennan, L., Ruckwied, K., Gerdes, K., 2016.
659 Structural, stratigraphic and sedimentological characterisation of a wide rift system: The Triassic
660 rift system of the Central Atlantic Domain. *Earth-Science Reviews* 158, 89-124.

661 Liu, L., Tang, D., Xu, H., Liu, L., 2016. Reservoir prediction of deep-water turbidite sandstones
662 with seismic lithofacies control - A case study in the C block of lower Congo basin. *Marine and*
663 *Petroleum Geology* 71, 1-11.

664 Loucks, R.G., Ruppel, S.C., 2006. Mississippian Barnett Shale: Lithofacies and depositional setting
665 of a deep-water shale-gas succession in the Fort Worth Basin, Texas. *Bulletin of the American*
666 *Association of Petroleum Geology* 91, 579-601.

667 Lowe, D.R., 1982. Sediment gravity flows II: depositional models with special reference to the
668 deposits of high-density turbidity currents. *Journal of Sedimentary Petrology* 52, 279–297.

669 Lundmark, A.M., Bue, E.P., Gabrielsen, R.H., Flaatt, K., Strand, T., Ohm, S.E., 2014. Provenance of
670 late Palaeozoic terrestrial sediments on the northern flank of the Mid North Sea High: detrital zircon
671 geochronology and rutile geochemical constraints. In: Scott, R.A., Smyth, H.R., Morton, A.C.,
672 Richardson, N. (Eds), *Sediment Provenance Studies in Hydrocarbon Exploration and Production*.
673 Geological Society of London, Special Publications 386, 243–259.

674 Meulenkamp, J.E., 1979. Field guide to the Neogene of Crete. In: Symeonidis, N., Papanikolaou, D.,
675 Dermitzakis, M. (Eds.), Field guide to the Neogene of Crete. Publications of the Department of
676 Geology and Paleontology of the University of Athens, Series A 32, 1–32.

677 Micaleff, A., Mountjoy, J.J., 2011. A topographic signature of a hydronamic origin for submarine
678 gullies. *Geology* 39, 115-118.

679 Mohriak, W.U., Leroy, S., 2013. Architecture of rifted continental margins and break-up evolution:
680 insights from the South Atlantic, North Atlantic and Red Sea–Gulf of Aden conjugate margins. In:
681 Mohriak, W.U., Danforth, A., Post, P.J., Brown, D.E., Tari, G.C., Nemčok, M., Sinha, S.T. (Eds.),
682 Conjugate Divergent Margins. Geological Society of London, Special Publications 369, 497-535.

683 Oçakoğlu, N., Demirbağ, E., Kuşçu, I., 2005. Neotectonic structures in İzmir Gulf and surrounding
684 regions (western Turkey): Evidences of strike-slip faulting with compression in the Aegean
685 extensional regime. *Marine Geology* 219, 155-171.

686 Ogata, K., Mutti, E., Pini, G.A., Tinterri, R., 2012. Mass transport-related stratal disruption within
687 sedimentary mélanges: examples from the northern Apennines (Italy) and south-central Pyrenees
688 (Spain). *Tectonophysics* 568, 185-199.

689 Papazachos, B.C., Karakostas, V.G., Papazachos, C.B., Scordilis, E.M., 2000. The geometry of the
690 Wadati-Benioff zone and lithospheric kinematics in the Hellenic arc. *Tectonophysics* 319, 275-300.

691 Pearce, F.D., Rondenay, S., Sachpazi, M., Charalampakis, M., Royden L.H., 2012. Seismic
692 investigation of the transition from continental to oceanic subduction along the western hellenic
693 subduction zone. *Journal of Geophysical Research* 117, B07306, doi:10.1029/2011JB009023.

694 Peters, J.M., 1985. Neogene and Quaternary vertical tectonics in the southern Hellenic arc and their
695 effect on concurrent sedimentation processes. Doctoral Thesis, Universiteit van Amsterdam, GUA
696 Papers in Geology Series 1, no. 23, 247 pp .

697 Postma, G., 1990. Depositional architecture and facies of river and fan deltas: a synthesis. In:
698 Colella, A., Prior, D.B. (Eds), *Coarse-Grained Deltas*, Vol 10, Blackwell Publishing Ltd, Oxford,
699 13-28.

700 Postma, G., Drinia, H., 1993. Architecture and sedimentary facies evolution of a marine, expanding
701 outer-arc half-graben (Crete, late Miocene). *Basin Research* 5, 103–124.

702 Postma, G., Fortuin, A.R., van Wamel, W.A., 1994. Basin-fill patterns controlled by tectonics and
703 climate: the Neogene ‘fore-arc’ basins of eastern Crete as a case history. In: Frostick, L.E., Steel,
704 R.J. (Eds), *Tectonic Controls and Signatures in Sedimentary Successions*, Blackwell Publishing
705 Ltd., Oxford, 335–362.

706 Riedel, M., Hing, J.K., Jin, Y.K., Rohr, K.M.M., Cote, M.M., 2016. First results on velocity
707 analyses of multichannel seismic data acquired with the icebreaker Araon across the southern
708 Beaufort Sea, offshore Yukon. *Geological Survey of Canada, Current Research* 2016-3, Natural
709 Resources Canada, pp. 27. Doi: 10.4095/298840.

710 Robertson, A.H.F., 2000. Mesozoic-Tertiary Tectonic-Sedimentary Evolution of a South Tethyan
711 Oceanic Basin and its Margins in Southern Turkey. In: Bozkurt, E., Winchester, J.A., Piper, J.D.A
712 (Eds), *Tectonics and Magmatism in Turkey and the Surrounding Area*. Geological Society of
713 London, Special Publications 173, 97-138.

714 Romer, R. L., Völs, S., Schulz, B., Xypolias, P., Zulauf, G., Krenn, E., 2008. Metamorphism of the
715 pre-Alpine basement and the Phyllite-Quartzite Units of the strait of Kythira (External Hellenides,
716 Greece). *Zeitschrift der Deutschen Geologischen Gesellschaft* 159, 469–483.

717 Sachpazi, M., Laigle, M., Charalampakis, M., Diaz, J., Kissling, E., Gesret, A., Becel. A., Flueh, E.,
718 Miles, P., Hirn, A., 2016. Segmented Hellenic slab rollback driving Aegean deformation and
719 seismicity. *Geophysical Research Letters* 43, 651-658.

720 Shaw, B., Jackson, J., 2010. Earthquake mechanisms and active tectonics of the Hellenic subduction
721 zone. *Geophysical Journal International* 181, 966-984.

722 Scheibner, C., Reijmer, J.J.G, Marzouk, A.M., Speijer, R.P., Kuss, J., 2003. From platform to basin:
723 The evolution of a Paleocene carbonate margin (Eastern Desert, Egypt). *International Journal of*
724 *Earth Sciences* 92, 624-640.

725 Schildgen, T.F., Cosentino, D., Caruso, A., Buchwaldt, R., Yildirim, C., Bowring, S.A., Rojay, B.,
726 Echtler, H., Strecker, M.R., 2012. Surface expression of eastern Mediterranean slab dynamics:
727 Neogene topographic and structural evolution of the southwest margin of the Central Anatolian
728 Plateau, Turkey. *Tectonics* 31, TC2005, doi:10.1029/2011TC003021.

729 Seyitoğlu, G., Scott, B., 1991. Late Cenozoic crustal extension and basin formation in west Turkey.
730 *Geological Magazine* 128, Issue 2, 155-166.

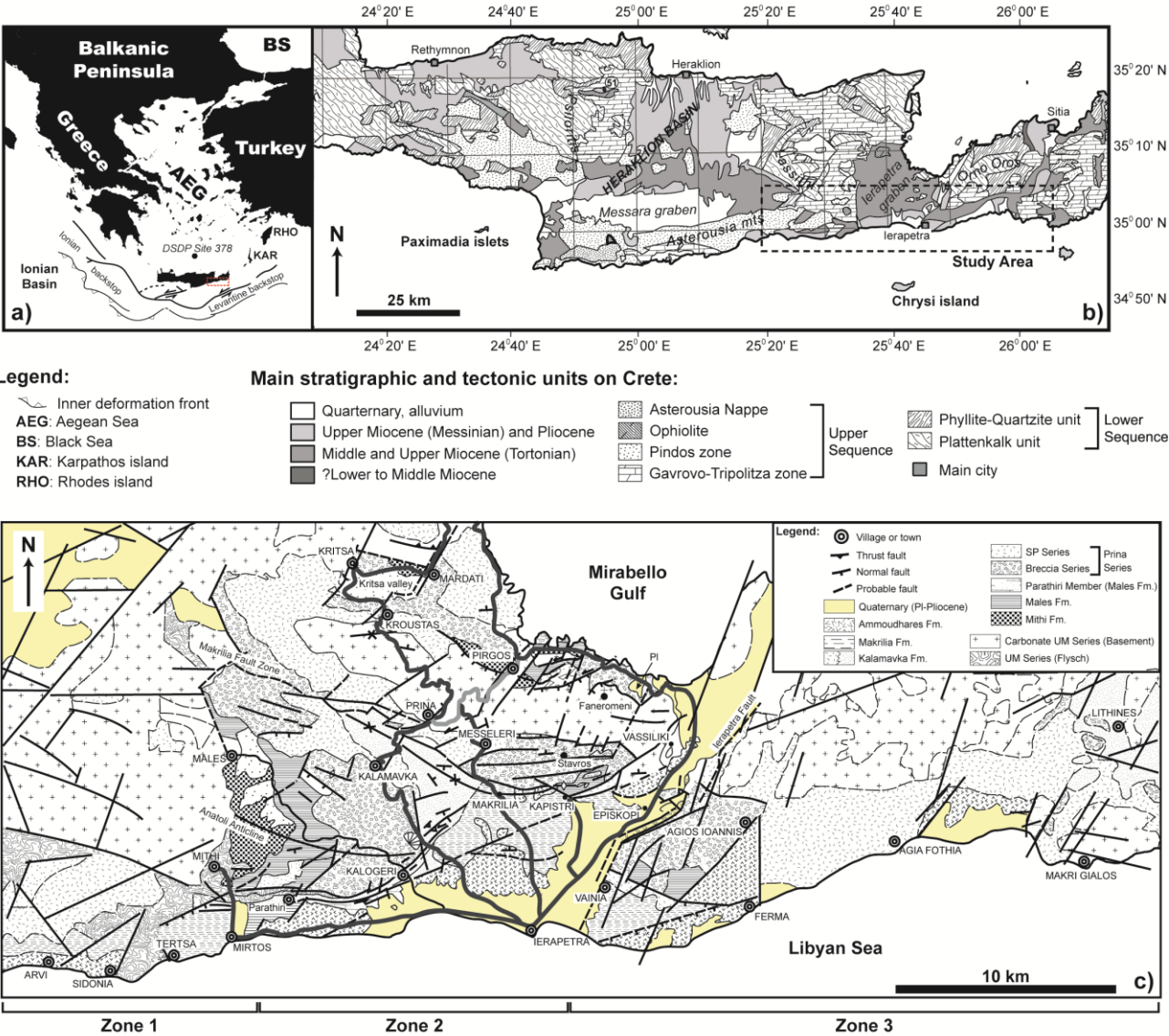
731 Soares, D.M., Alves, T.M., Terrinha, P., 2012. The breakup sequence and associated lithospheric
732 breakup surface: Their significance in the context of rifted continental margins (West Iberia and
733 Newfoundland margins, North Atlantic). *Earth Planetary Science Letters* 355, 311-326.

734 Stampfli, G.M., 2000. Tethyan oceans. In: Bozkurt, E., Winchester, J.A. and Piper, J.D.A (Eds).
735 *Tectonics and Magmatism in Turkey and the Surrounding Area*. Geological Society of London,
736 *Special Publications* 173, pp. 1-23.

737 ten Veen, J.H., Postma, G., 1999. Neogene tectonics and basin fill patterns in the Hellenic outer-arc
738 (Crete, Greece). *Basin Research* 11, 223–241.

739 Thomson, S.N., Stöckhert, B., Brix, M.R., 1999. Miocene high-pressure metamorphic rocks of
740 Crete, Greece, rapid exhumation by buoyant escape. In: Ring, U., Brandon, M.T., Lister, G.S.,
741 Willett, S.D. (Eds.), *Exhumation Processes, Normal Faulting, Ductile Flow and Erosion*. Geological
742 *Society of London, Special Publications* 154, 87–107.

743 Tomás, S., Zitzmann, M., Homann, M., Rumpf, M., Amour, F., Benisek, M., Marcano, G., Mutti,
 744 M., Betzler, C., 2010. From ramp to platform: building a 3D model of depositional geometries and
 745 facies architectures in transitional carbonates in the Miocene, northern Sardinia. *Facies* 56, 195-210.
 746 van Hinsbergen, D.J.J., Meleunkamp, J.E., 2006. Neogene supradetachment basin development on
 747 Crete (Greece) during exhumation of the South Aegean core complex. *Basin Research* 18, 103–124.
 748 Wilson, M.E.J., Bosence, D.W.J., Limborg, A., 2000. Tertiary syntectonic carbonate platform
 749 development in Indonesia. *Sedimentology* 47, 395-419.
 750 Wilson, R.C.L., Manatschal, G., Wise, S., 2001. Rifting along non-volcanic passive margins:
 751 stratigraphic and seismic evidence from the Mesozoic successions of the Alps and western Iberia. In:
 752 Wilson, R.C.L., Whitmarsh, R.B., Taylor, B., Froitzheim, N. (Eds), *Non-Volcanic Rifting of*
 753 *Continental Margins: A Comparison of Evidence from Land and Sea*. Geological Society of London,
 754 Special Publications 187, pp. 429-452.
 755 Zachariasse, W.J., van Hinsbergen, D.J.J., Fortuin, A.R., 2008. Mass wasting and uplift on Crete
 756 and Karpathos during the early Pliocene related to initiation of south Aegean left-lateral, strike-slip
 757 tectonics. *Bulletin of the Geological Society of America* 120, 976–993.
 758



760 Figure 1

761 Fig. 1. Regional geological map of the southern Cretan margin highlighting: (a) the relative location

762 of Crete in relation to the Aegean Sea, Greek and Turkish landmasses; (b) the regional geology of

763 Crete and of the study area (modified from Postma et al., 1993). (c) Geological map of the study

764 area in SE Crete.

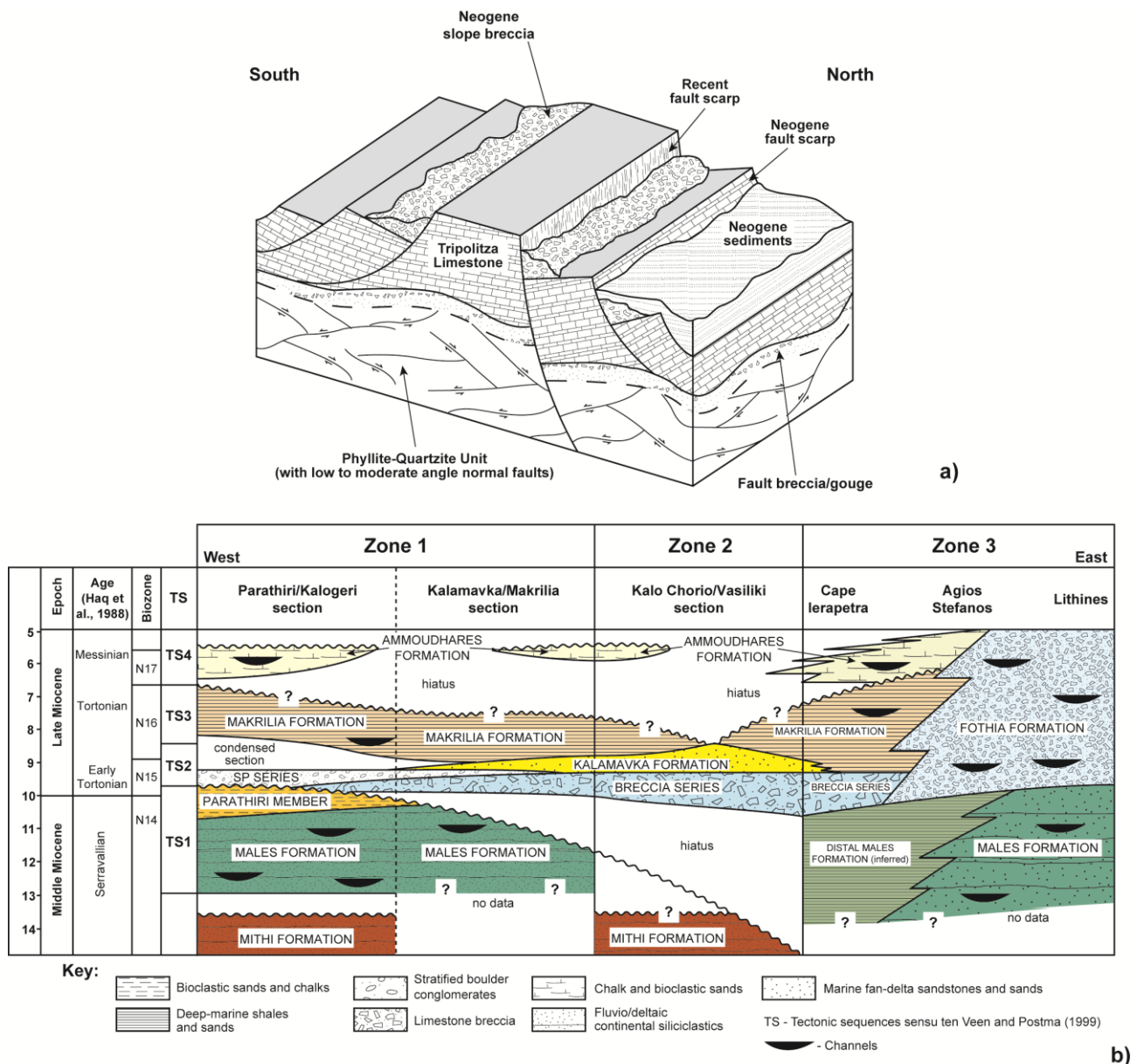


Figure 2

Fig. 2. Schematic diagrams illustrating the tectono-sedimentary evolution of Crete in the late Cenozoic. (a) Three-dimensional sketch summarising the extensional character of the studied area in Crete. Modified from Thomson et al., 1998; Kokinou et al., 2012. (b) Principal lithological units in the Ierapetra region and southern Crete. Lithological units in Zones 1 and 2 units, based on Postma and Drinia (1993), are compared in this figure with their counterparts to the East of Ierapetra (Zone 3) and with the Tectonic Sequences of Ten Veen and Postma (1999), which are described in this paper.

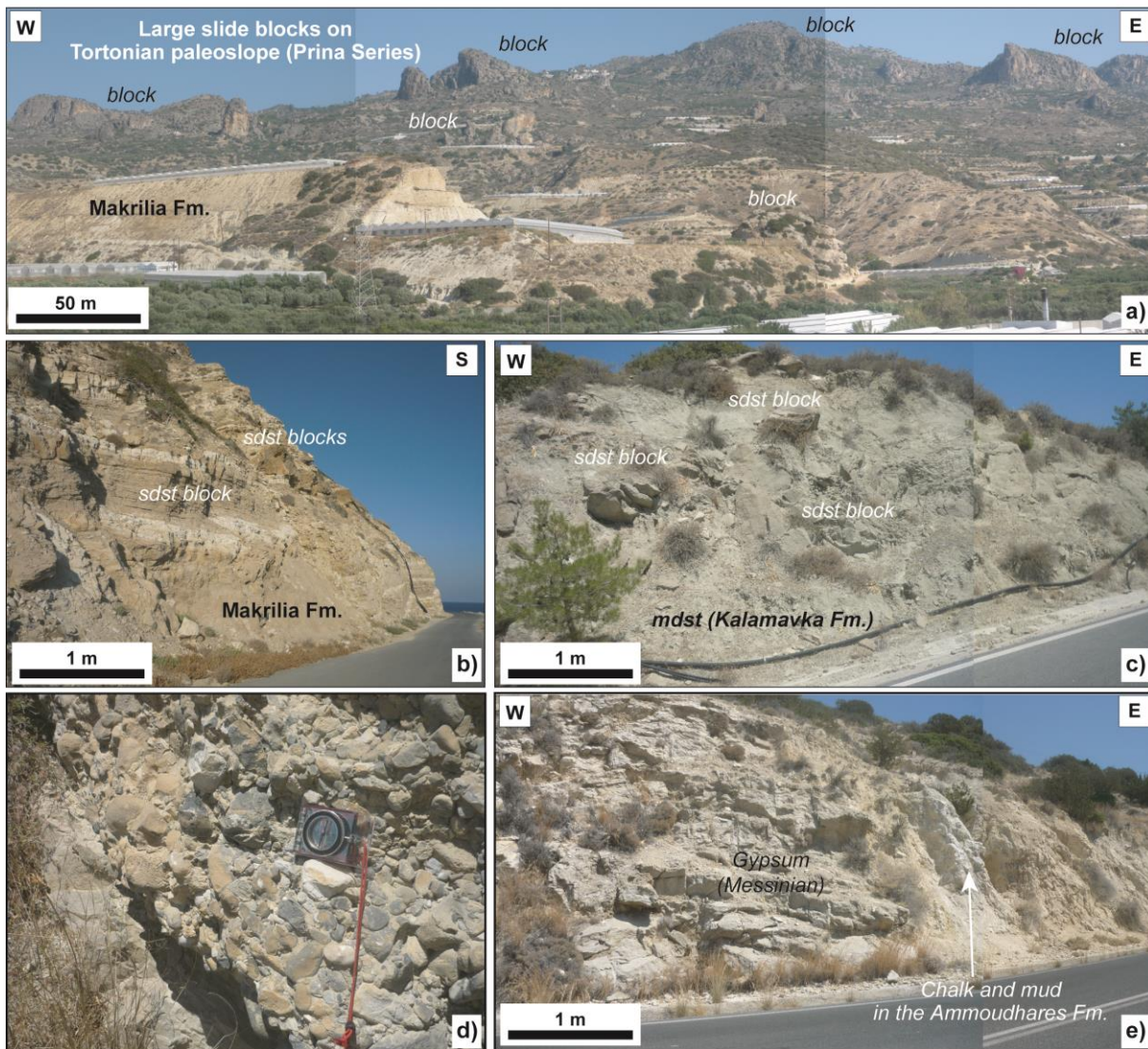


Figure 3

Fig. 3. Outcrop examples of facies associations as defined by Postma and Drinia (1993). (a) Fa 2-4; allochthonous slide blocks in Zone 2, over the paleoslope bordering the Ierapetra Graben to the northeast (Anatoli-Kalamavka region; Figures 1c and 5). (b) Fa A; example of channel-fill deposits in Zone 2, which are sandier and less erosive than in Zone 1, Location 50 in Figure 5. (c) Fa 1, strata belonging to the Males Formation in slope strata (unit t in Figure 5) outcropping around Anatoli (location 23, Fig. 5). (d) Fa 2-4, detail of boulder-conglomerate facies in proximal parts of the paleoslope in Zone 2 (unit pr in Figure 5). (e) Messinian evaporites, not included in Postma and Drinia (1993) facies associations and comprising mostly blocky and cavernous salt, outcropping close to Ammoudhares at location 48, Figure 5.

785



786

Figure 4 -

787

Fig. 4. Detail of facies associations A to C as observed at coastal outcrops. The photo shows

788

interbedded with slope turbidites in the upper part of the Makrilia Formation at Sidonia, Zone 1.

789

Location 73, Figure 4.

790

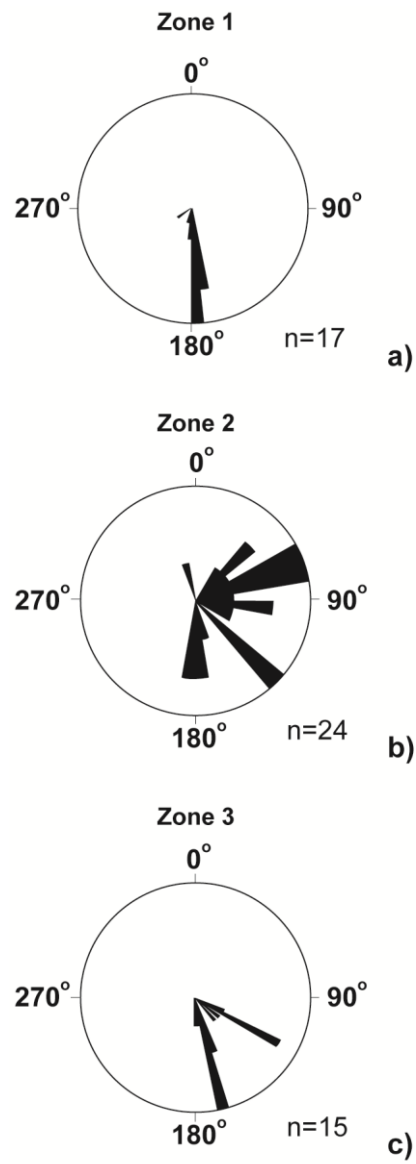


Figure 5

791

792 Fig. 5. Paleocurrent indicators acquired in: (a) Zone 1, (b) Zone 2, and (c) Zone 3.

793

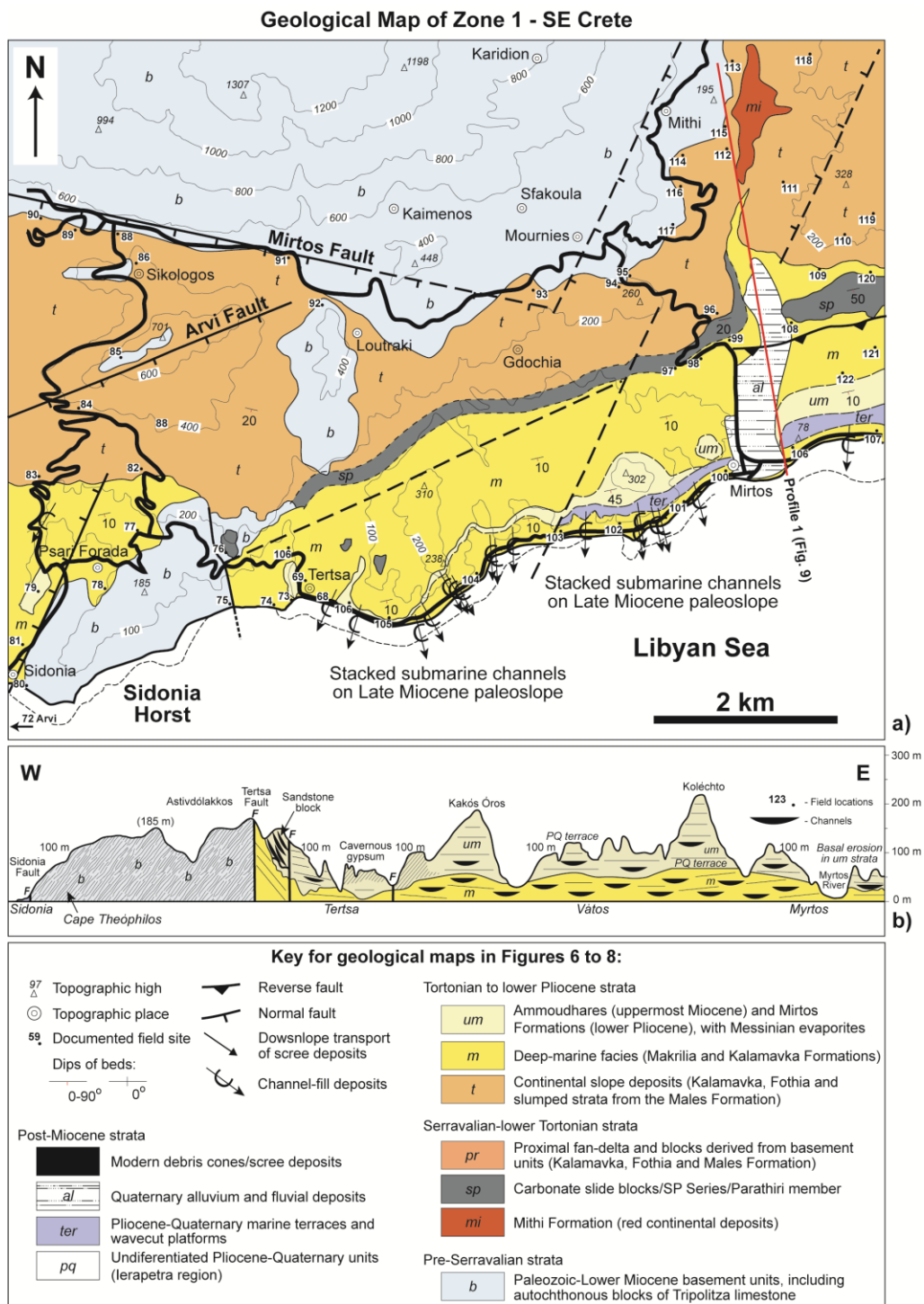


Figure 6

Fig. 6. (a) Geological map of Zone 1, located between the village of Myrtos and Sidonia/Arvi, and (b) regional transect along coastal outcrops in Zone 1. The figure also shows the key for the geological maps in Figures 6 to 8. The location of lithological profile 1 in Figure 9 is also highlighted in the geological map in a).

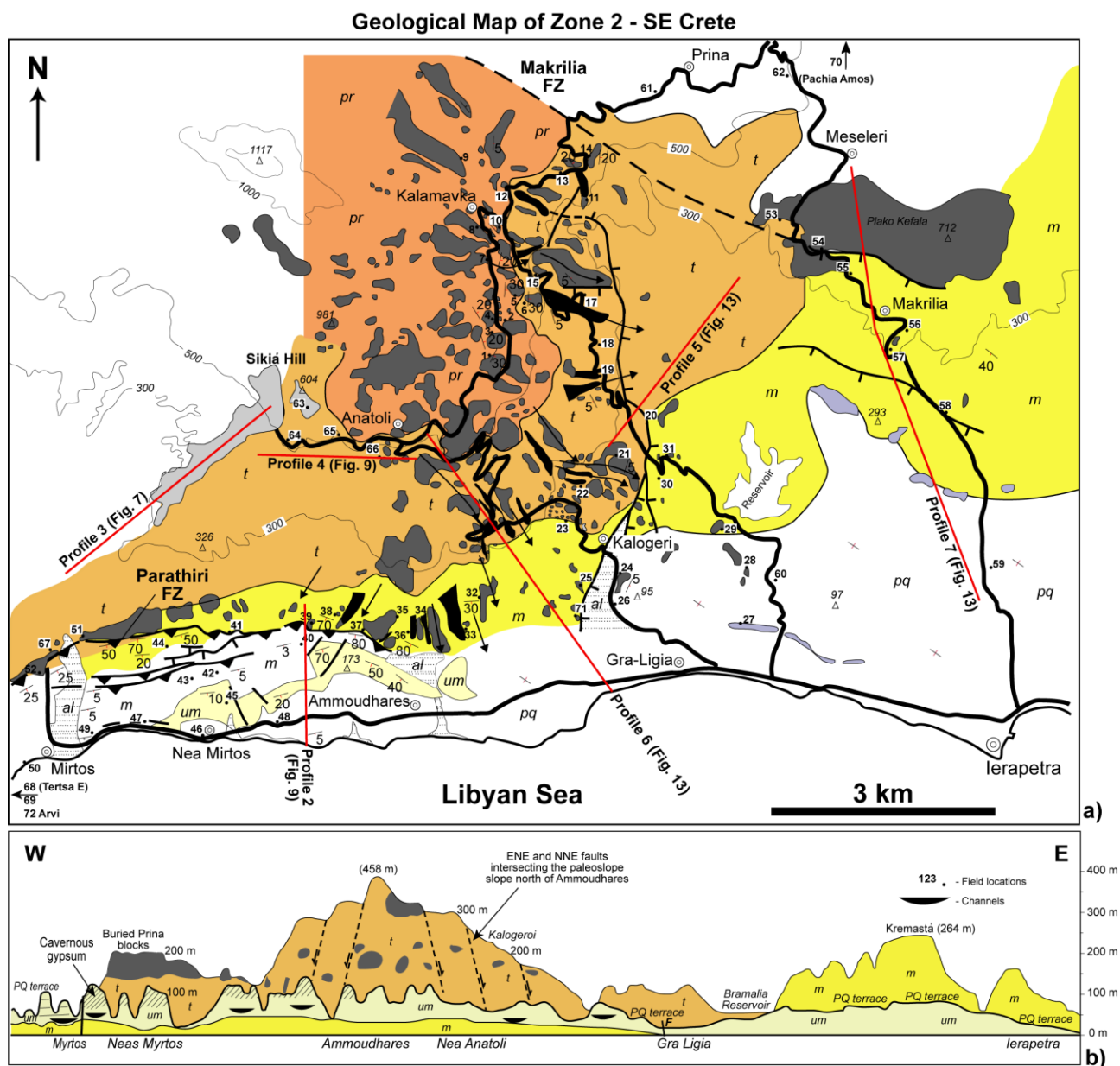


Figure 7

Fig. 7. (a) Geological map of Zone 2, located in the southern and central parts of the Ierapetra Graben and paleoslopes to the northwest and north. (b) Regional transect along coastal outcrops in Zone 2. The locations of lithological profiles 2 to 7, shown in Figures 9 and 13, are also highlighted in the geological map in a). Key given in Figure 6.

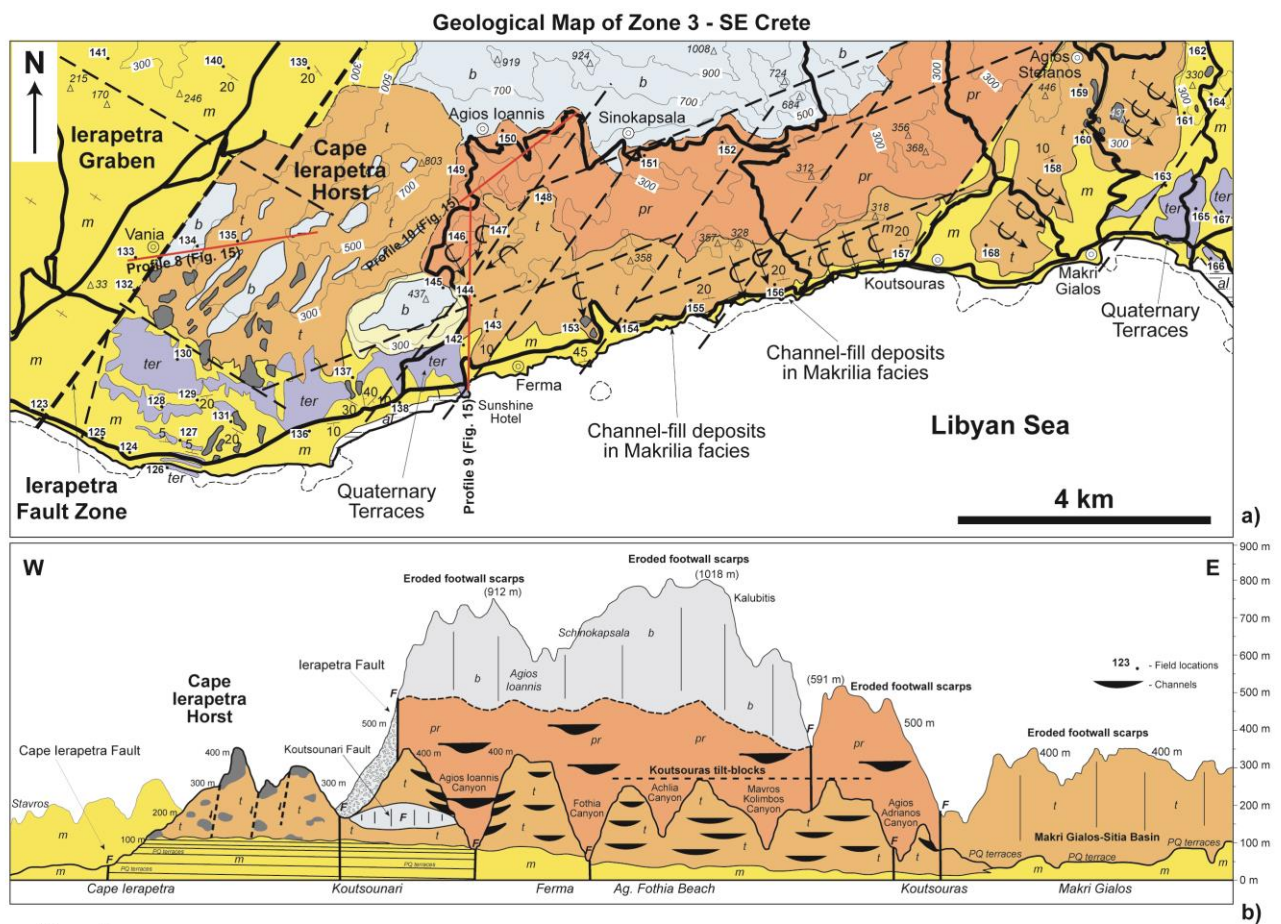


Figure 8

Fig. 8. (a) Geological map of Zone 3, located to the east of the Ierapetra Graben. (b) Regional transect along coastal outcrops in Zone 3. The locations of lithological profiles 8 to 10 in Figure 13 are shown in the geological map in a). Key given in Figure 6.

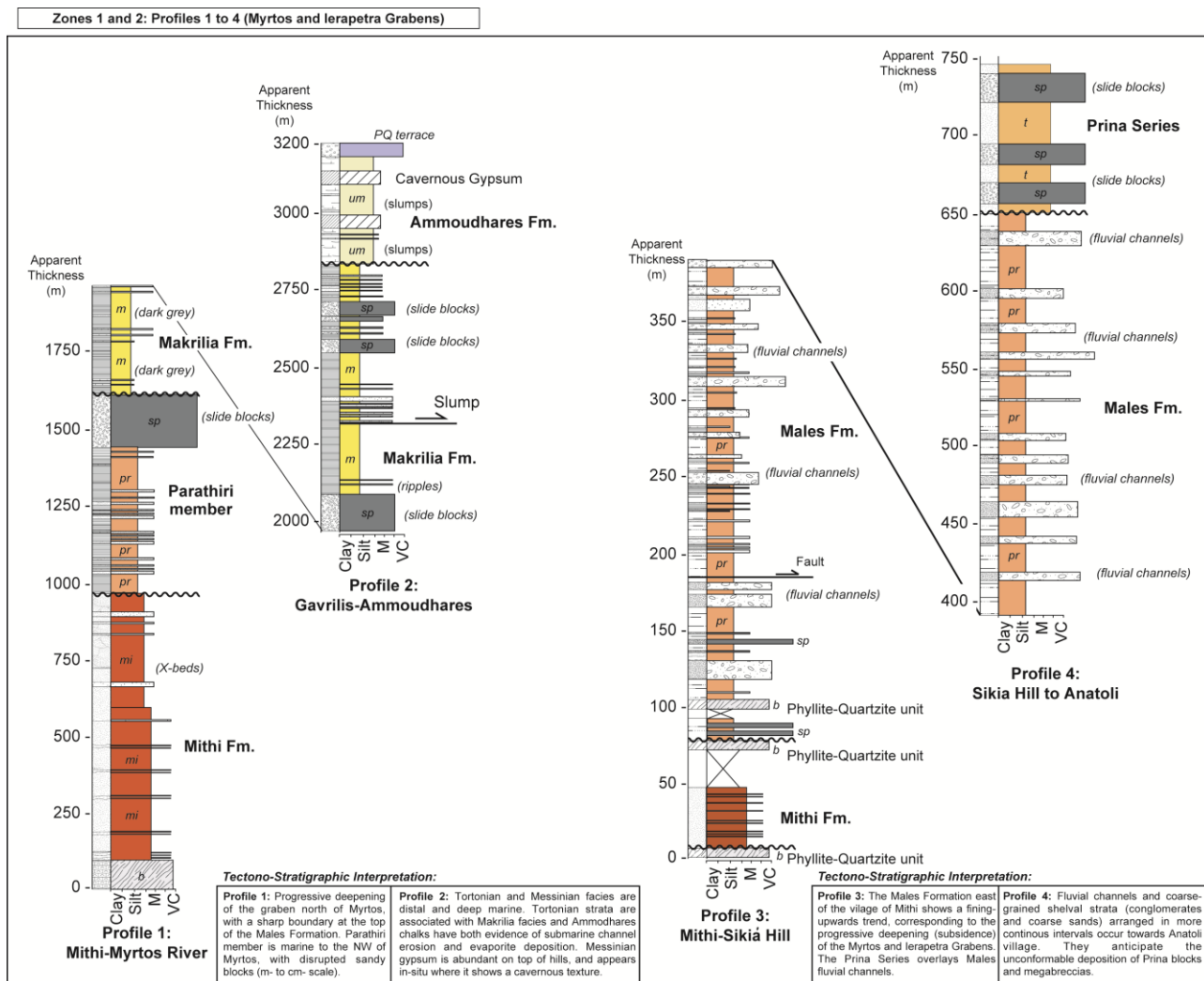


Figure 9

Fig. 9. Lithological profiles 1 to 3 across Zone 1, as shown on the map in Figure 6.

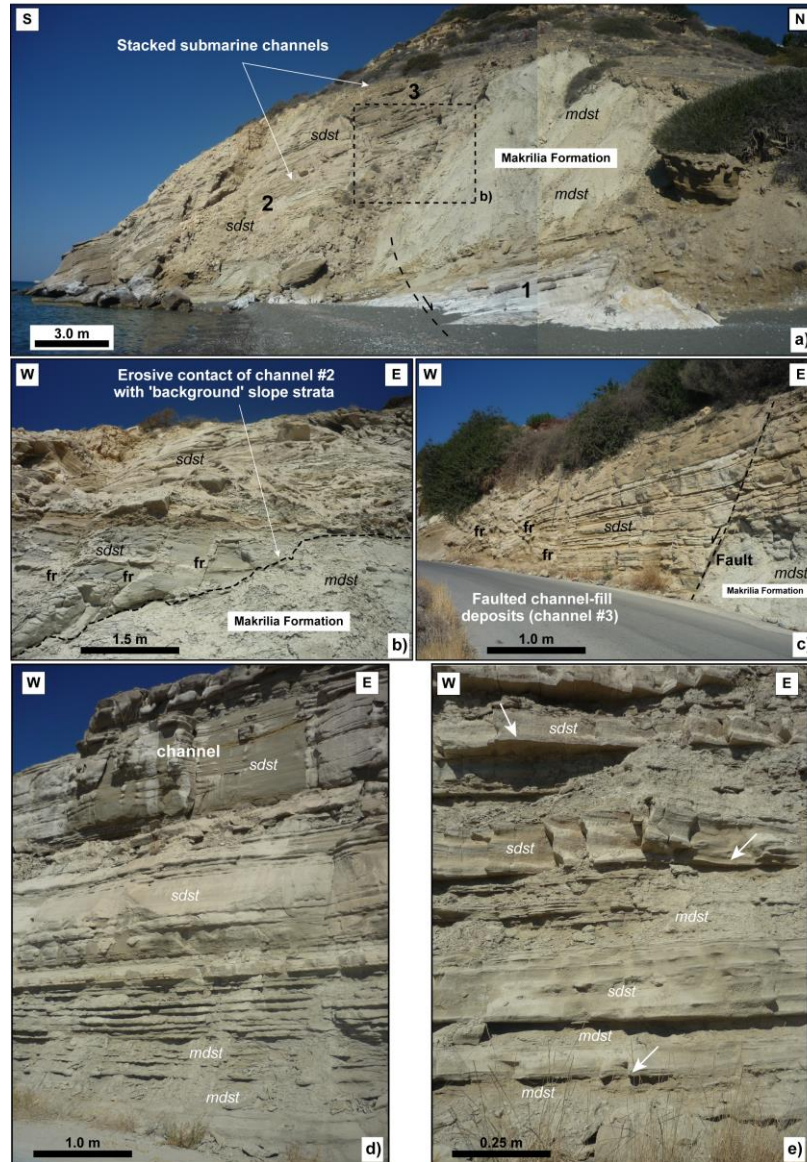


Figure 10

816

817 Fig. 10. Field photographs highlighting the depositional facies, tectonic sequences and stratigraphic

818 formations of the study area. (a) Stacked submarine channels in Sidonia (location 80, Fig. 6), within

819 uppermost Makrilia Formation strata. (b) Detail of the erosive contact between one of the channel-

820 fill deposits at Sidonia (channel #2, location 80) and mudstones in the Makrilia Formation. (c) The

821 top of the Makrilia Formation is marked at Sidonia by wider channel-fill deposits, and sandy

822 overbank strata. (d) Example of turbidite sands and mudstones in the Makrilia Formation in location

823 103, west of Myrtos (see Fig. 6). (e) Example in location 102 of submarine fan deposits, with minor

824 sequences of and larger amounts of mudstone when compared with channel-fill deposits. sdst-

825 sandstone; mdst-mudstone.

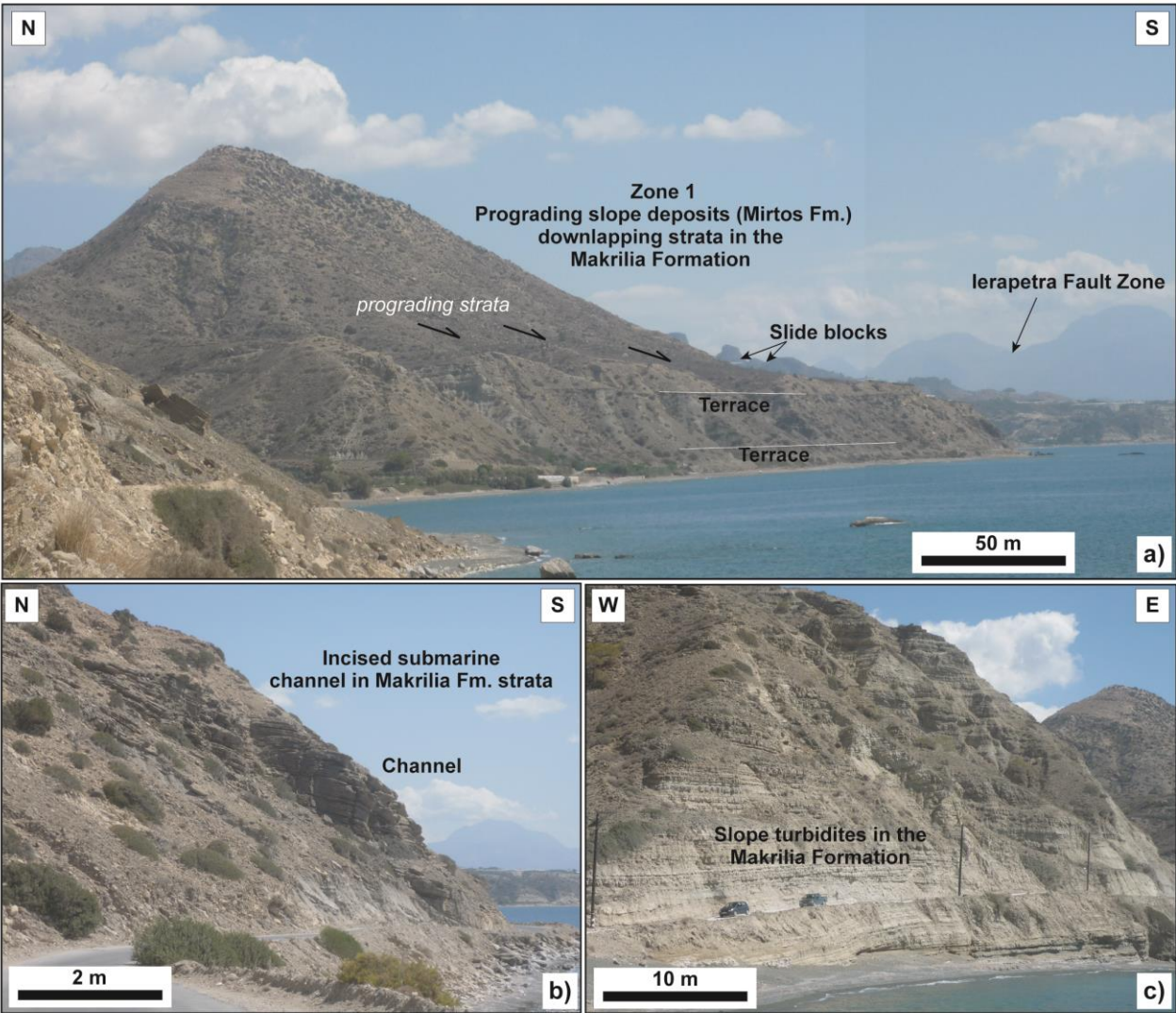


Figure 11

Fig. 11. (a) Sub-horizontal Makrilia strata are downlapped by early Pliocene strata in the Myrtos Formation (Table 1), Location 101 in Figure 6. (b) Detail of submarine channel-fill deposits in Tertsia, Zone 1, location 106 (Fig. 6). (c) Detail of slope and submarine-fan strata deposited on the late Miocene paleoslope in Zone 1 (location 102, Fig. 6).



Figure 12

833

834 Fig. 12. Section showing (a) slumped continental-slope turbidites part of the uppermost Makrilia
 835 and Ammoudhares Formations, Arvi, and (b) interpretation of strata displacement (location 72, Fig.
 836 5).

837

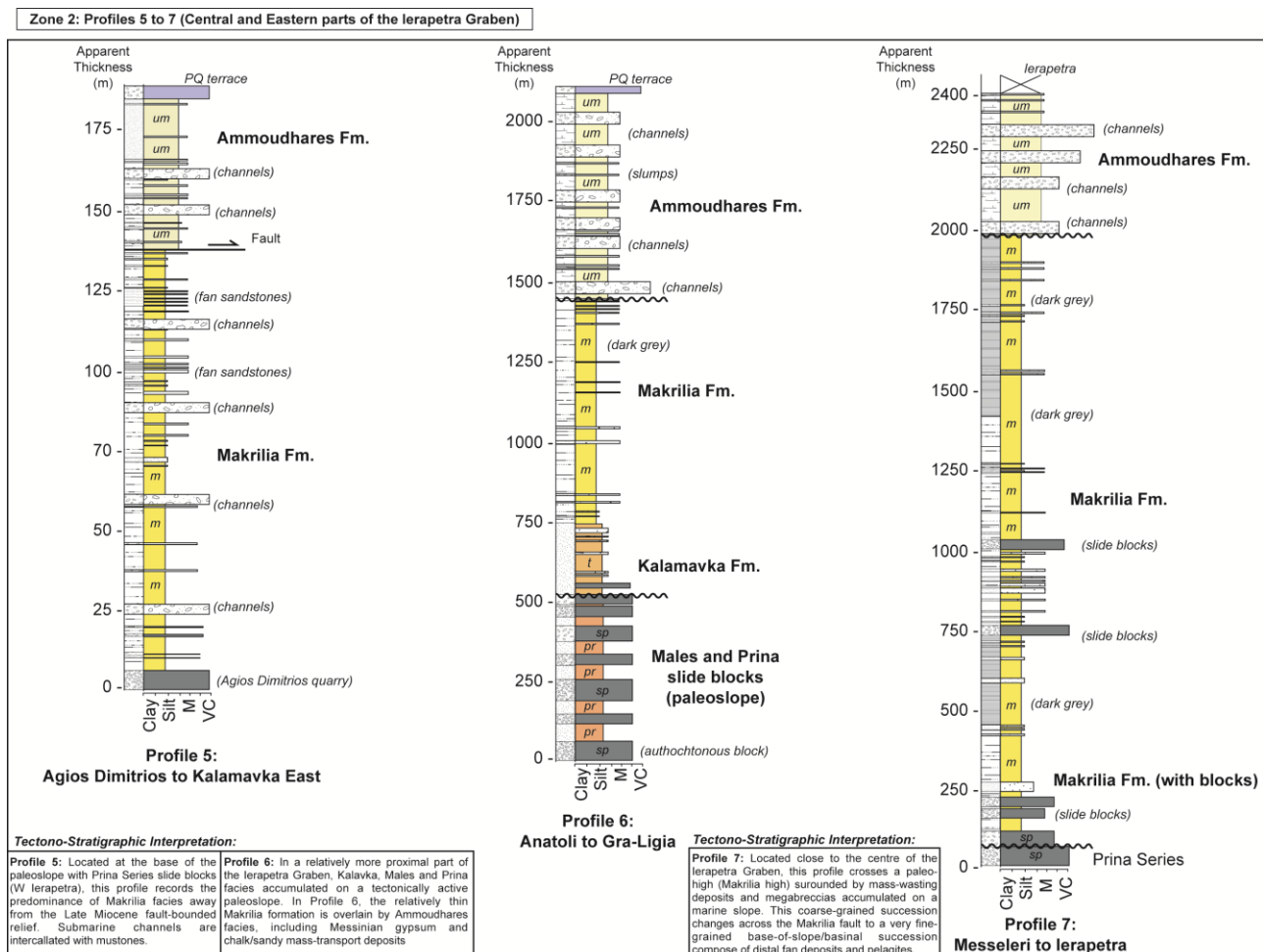


Figure 13

Fig. 13. Lithological profiles 5 to 7 across Zone 2, as shown on the map in Figure 7

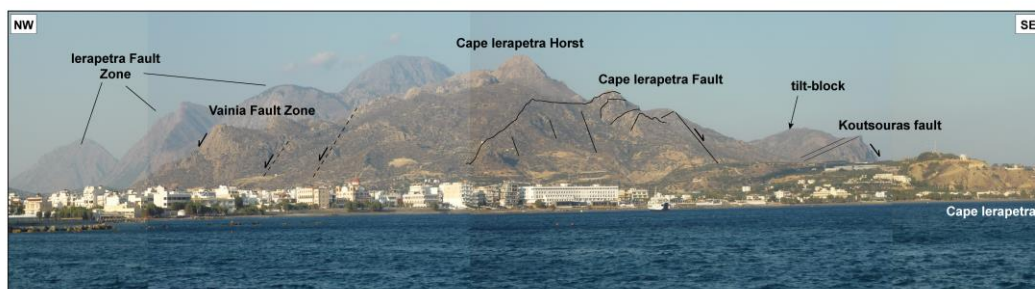
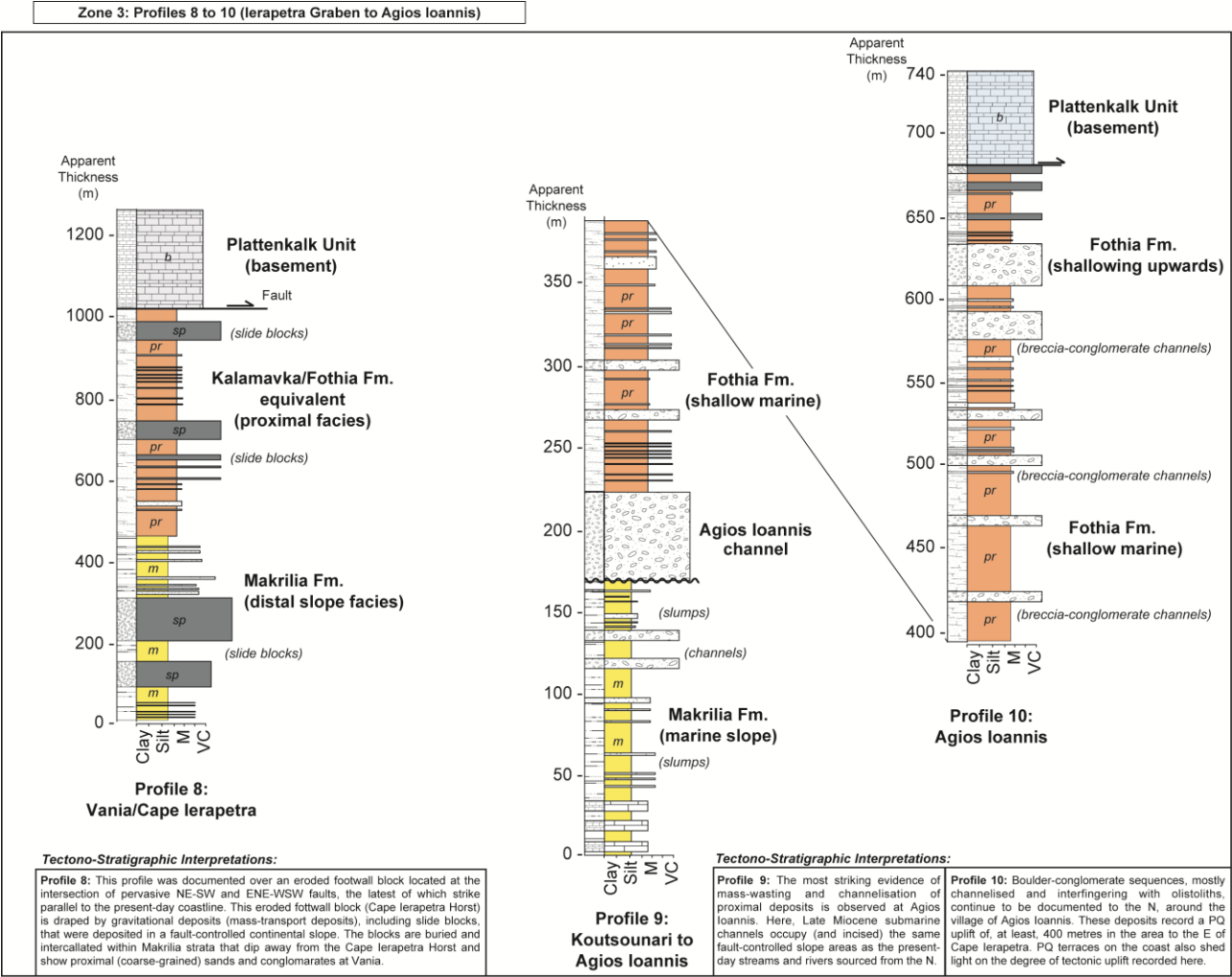


Figure 14

Fig. 14. Panoramic view of the Cape Ierapetra Horst and associated fault zones from Ierapetra, SE Crete. The photo mosaic shows the Fothia Formation at the zone of intersection of faults trending N20oE and N70oE.

845



846

Figure 15

847

Fig. 15. Lithological profiles 8 to 10 across Zone 3, as shown on the map in Figure 8.

848

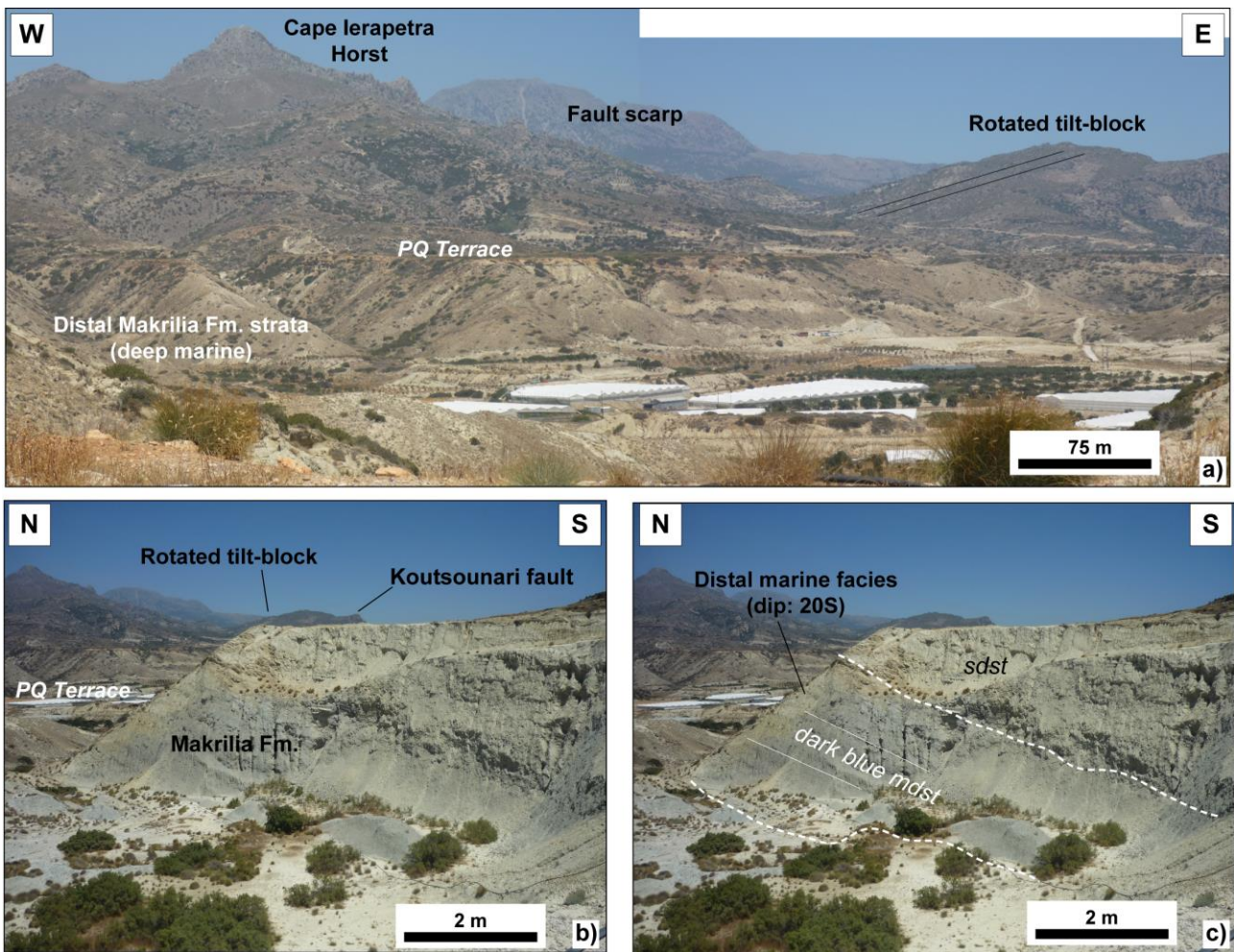


Figure 16 -

Fig. 16. (a) View of strata at Cape Ierapetra, where Makrilia Formation sediments predominates together with uplifted Pliocene-Quaternary terraces and rotated tilt-blocks (location 128, Fig. 8). (b) Example of distal Makrilia Formation facies here composed of dark-blue shales and minor sand intervals. Location 129, Figure 8. (c) Interpretation of lithologies, inferred boundaries and strata dips in the same outcrop location in b). sdst-sandstone; mdst-mudstone.

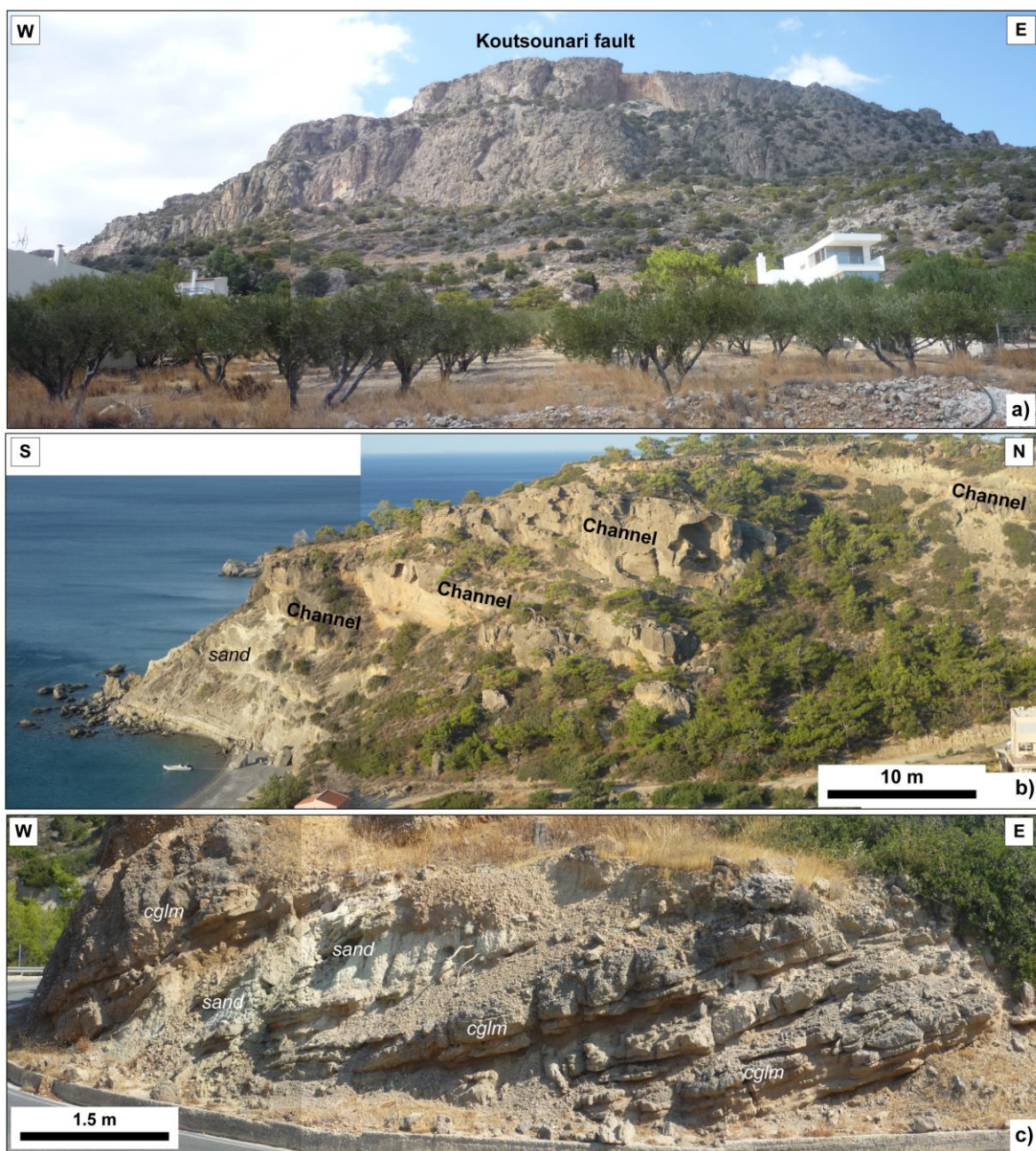


Figure 17

Fig. 17. (a) Panoramic view of the Koutsounari fault in Zone 3, and associated fan delta deposits accumulated on its toe. Location 138, Figure 6. (b) Continental fan-delta deposits give way to channel-fill deposits and distal fan-delta (pro-delta?) deposits on coastal outcrops. Location 153, Figure 8. (c) Example of channel-fill deposits at location 154 (Fig. 8) composed of poorly consolidated conglomerates interbedded in marine sands and muds.

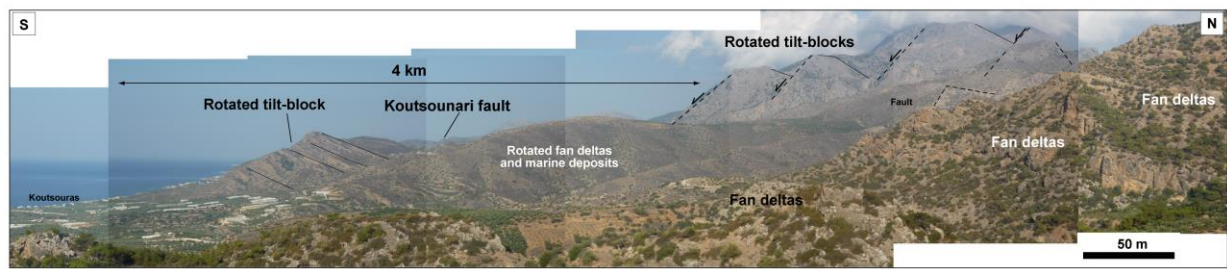


Figure 19

863

864 Fig. 18. a) Panoramic view from the eastern part of Zone 3, from Agios Stefanos (location 158, Fig.
 865 8). The photomosaic highlights the geometry of E-W half-grabens where proximal deposits (fan
 866 deltas and shallow marine strata) change abruptly into more distal marine facies along the present-
 867 day coastline.

868



Figure 19

869

870 Fig. 19. Detail of channel-fill units at Agios Ioannis, location 146 in Zone 3 (Fig. 8), sourced from
 871 the Cape Ierapetra Horst and footwall blocks to the north.

872

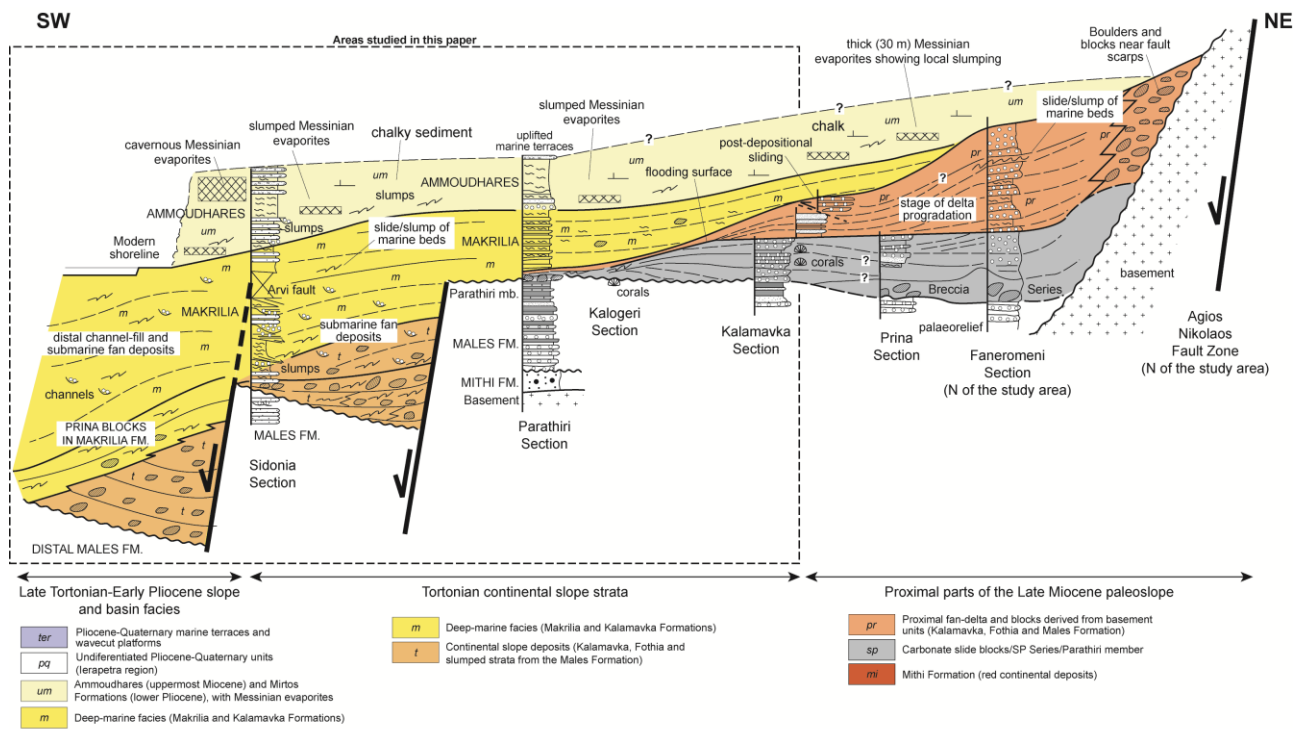


Figure 20

Fig. 20. Architecture of fault-bounded basins deposited SE Crete during the late Serravallian–Messinian, from NE to SW across Zones 1 and 3.

877

Tectono-Sedimentary Unit (TS)	Age	Regional Stratigraphic Units	Sedimentological character and local tectonic evolution (ten Veen and Postma, 1999)
TS5	Late Messinian to Recent	Mirtos Formation and undifferentiated Quaternary terraces/alluvial fans	Shallow marine, estuarine, coastal, and deltaic deposits. Gradual deepening is recorded towards the top of the unit. No conspicuous faulting controlling basin fill.
TS4	Late Tortonian-Messinaian mostly moderately sloping	Uppermost Makrilia and Ammoudhares Formations	Bioclastic chalks and debrites interrupted by turbidites, calcarenites and marls. White, rich in sponge needles and evaporites.
TS3	Middle Tortonian	Makrilia and Upper Kalamavka Formations	Subsidence in N-S seaways with uplift of basin shoulders (and older strata). Stacked channel fill deposits and distal turbidites and shales.
TS2	Early Tortonian	Prina Series and lower Kalamavka Formation	Sudden influx of large masses of Tripolitza limestone breccias and blocks. Distal turbidites in starved basins recording very high subsidence rates
TS1	Late Serravalian	Parathiri Member	Shallow marine, estuarine, coastal, and deltaic deposits. Gradual deepening is recorded towards the top of the unit. No conspicuous faulting controlling basin fill.

878

879 Table 1. Summary table correlating the Late Miocene tectono-sedimentary (TS) units on Crete with
880 formal stratigraphic units and their lithological character. Tectono-sedimentary units are from ten
881 Veen and Postma (1993). Formation and member names are based on Fortuin (1977).